

YTHDF2 correlates with tumor immune infiltrates in lower-grade glioma

Xiangan Lin^{1,*}, Zhichao Wang^{2,*}, Guangda Yang^{2,*}, Guohua Wen², Hailiang Zhang²

¹Department of Cancer Chemotherapy, Sun Yat-Sen Memorial Hospital of Sun Yat-Sen University, Guangzhou 510000, China

²Department of Cancer Chemotherapy, Zengcheng District People's Hospital of Guangzhou, Guangzhou 511300, China

*Co-first authors

Correspondence to: Guangda Yang; email: yangguangda.123com@163.com; <https://orcid.org/0000-0003-4307-2517>

Keywords: YTHDF2, lower-grade glioma, biomarker, tumor-infiltrating, prognosis

Received: February 13, 2020

Accepted: July 20, 2020

Published: September 27, 2020

Copyright: © 2020 Lin et al. This is an open access article distributed under the terms of the [Creative Commons Attribution License](https://creativecommons.org/licenses/by/3.0/) (CC BY 3.0), which permits unrestricted use, distribution, and reproduction in any medium, provided the original author and source are credited.

ABSTRACT

Immunotherapy is an effective treatment for many cancer types. However, YTHDF2 effects on the prognosis of different tumors and correlation with tumor immune infiltration are unclear. Here, we analyzed The Cancer Genome Atlas and Gene Expression Omnibus data obtained through various web-based platforms. The analyses showed that YTHDF2 expression and associated prognoses may depend on cancer type. High YTHDF2 expression was associated with poor overall survival in lower-grade glioma (LGG). In addition, YTHDF2 expression positively correlated with expression of several immune cell markers, including PD-1, TIM-3, and CTLA-4, as well as tumor-associated macrophage gene markers, and isocitrate dehydrogenase 1 in LGG. These findings suggest that YTHDF2 is a potential prognostic biomarker that correlates with LGG tumor-infiltrating immune cells.

INTRODUCTION

Despite therapeutic advances in recent years, cancer still ranks as a leading cause of death [1]. The Cancer Genome Atlas (TCGA) program and Gene Expression Omnibus (GEO) data, which provide important information for further understanding of tumor biology, are available to users via multiple web-based platforms ([2–11]). This knowledge is essential and has already been incorporated into clinical practice, improving our ability to diagnose, treat, and prevent cancer.

Immunotherapy based on cytotoxic T lymphocyte-associated antigen 4 (CTLA4), programmed death-1 (PD-1), and programmed death ligand-1 (PD-L1) inhibitors has emerged as an effective treatment in melanoma and non-small-cell lung carcinoma [12, 13]. As noted in several studies, tumor-infiltrating lymphocytes, such as tumor-associated macrophages (TAMs),

play an important role in patient prognosis and the efficacy of immunotherapy [14–17]. Some markers have been identified as effectors of immunotherapy [18–20]. However, current immunotherapy strategies have shown poor clinical efficacy in other cancers [21–23]. Therefore, identifying efficacious immune-related therapeutic targets in cancers is urgently needed.

m6A is a prevalent internal mRNA modification [24, 25] and plays an important role in cancer progression [26] and immunoregulation [27]. m6A modification is regulated by “writers” (m6A methyltransferases, such as methyltransferase-like 3 [METTL3] and methyltransferase-like 14), “erasers” (m6A demethyltransferases, such as fat mass and obesity-associated [FTO] and alkB homologue 5, RNA demethylase), and “readers” (effectors recognizing m6A, such as three YTH domain proteins [YTHDF1–3]) [28]. m6A modification (deletion of METTL3 or YTHDF2) controls the innate immune

response to infection by targeting type I interferons [29]. m6A modification by FTO increases melanoma growth and decreases response to anti-PD-1 blockade immunotherapy [30]. METTL3-mediated mRNA m6A methylation promotes dendritic cell (DC) activation and function [31]. YTHDF1 shows anti-tumor immunity in DCs [32]. YTHDF2 sequesters m6A-circRNA and is essential for suppression of innate immunity [33]. In addition, YTHDF2 plays cell type-specific roles in lytic viral gene expression during Kaposi's sarcoma-associated herpesvirus infection [34]. YTHDF2 is a functional m6A-specific reader protein that mainly regulates stability of mRNA [35]. A previous study showed that YTHDF2 expression was regulated by miR-145 in hepatocellular carcinoma (HCC) cells [36]. Moreover, YTHDF2 may function as a tumor suppressor to inhibit cell proliferation and growth in HCC [37]. In addition, YTHDF2 acted as a tumor oncogene to promote prostate cancer cell proliferation and migration [38]. Interestingly, it has been found that YTHDF2 plays dual roles in pancreatic cancer cells by promoting proliferation and inhibiting migration and invasion [39]. Therefore, the roles of YTHDF2 in cancer remain elusive, especially regarding tumor-immune interactions.

In this study, we analyzed YTHDF2 expression and its correlation with the prognosis of cancer patients via a pan-cancer analysis using various web-based platforms. We also investigated the relationship between YTHDF2 expression and tumor-infiltrating immune cells (TIICs) in various cancers. Moreover, we analyzed the correlation of YTHDF2 with isocitrate dehydrogenase 1 (IDH1) in LGG. Finally, we performed the enrichment analysis of YTHDF2 in LGG. These results shed light on the important role of YTHDF2 in LGG and provide an underlying mechanism between YTHDF2 and tumor-immune interactions.

RESULTS

YTHDF2 expression in cancer

We used the Tumor Immune Estimation Resource (TIMER) database to study differences in YTHDF2 expression in tumor tissues and adjacent normal tissues. Figure 1A shows that YTHDF2 expression was substantially higher in BLCA (bladder urothelial carcinoma), breast invasive carcinoma, colon adenocarcinoma, esophageal carcinoma, LUAD (lung adenocarcinoma), stomach adenocarcinoma, prostate adenocarcinoma, and UCEC (uterine corpus endometrial carcinoma) tissues than in adjacent normal tissues. However, YTHDF2 expression was lower in head and neck squamous cell carcinoma, KICH (kidney chromophobe), KIRC (kidney renal clear cell carcinoma), kidney renal papillary cell carcinoma, and LIHC (liver

hepatocellular carcinoma) tissues than in adjacent normal tissues. YTHDF2 expression was not expressed substantially between cholangiocarcinoma, lung squamous cell carcinoma, READ (rectum adenocarcinoma), and thyroid carcinoma tissues and adjacent normal tissues. Unfortunately, no data were available on YTHDF2 expression in adjacent normal tissues for the following cancers: adrenocortical carcinoma, DLBC (lymphoid neoplasm diffuse large B-cell lymphoma), GBM (glioblastoma multiforme), LAML (acute myeloid leukemia), LGG (lower-grade glioma), mesothelioma, OV (ovarian serous cystadenocarcinoma), PAAD (pancreatic adenocarcinoma), pheochromocytoma and paraganglioma, SARC (sarcoma), skin cutaneous melanoma, testicular germ cell tumor, thymoma, uterine carcinosarcoma, and uveal melanoma.

To provide a more comprehensive evaluation of YTHDF2 expression in cancers, we used the online database Gene Expression Profiling Interactive Analysis (GEPIA) to compare YTHDF2 expression across 33 TCGA cancer types and in TCGA and GTEx normal tissues. Figure 1B shows that YTHDF2 expression was elevated in many cancers, especially DLBC, GBM, PAAD, and THYM.

We then used the ONCOMINE database to compare YTHDF2 expression in human cancer and corresponding normal samples (Figure 1C and Supplementary Table 1). Supplementary Table 1 ([40–46]) shows YTHDF2 datasets in human cancers. YTHDF2 expression upregulated in anaplastic oligoastrocytoma, with a fold change of 2.433, and downregulated in glioblastoma, with a fold change of -2.762. In addition, YTHDF2 expression upregulated in the other cancers, with a fold change from 2.038 to 11.69.

Prognostic value of YTHDF2 in cancer

We investigated the impact of YTHDF2 expression on survival rates by using the PrognScan database. The relationships between YTHDF2 expression and prognosis in different cancers are shown in Supplementary Table 2. YTHDF2 expression substantially impacted the prognosis of four cancer types, including brain, breast, colorectal, and soft tissue. However, the impact of YTHDF2 on survival was conflicting in two independent breast cancer cohorts.

To further predict the prognostic potential of YTHDF2 in cancers, four databases (GEPIA, TIMER, OncoLnc, and Kaplan-Meier plotter) were used to evaluate the prognostic value of YTHDF2. The detailed results are summarized in Supplementary Table 3. In the GEPIA database, high YTHDF2 expression was associated with poorer overall survival (OS) and disease-free survival

(DFS) in KICH (OS hazard ratio [HR] = 9.2, P= 0.011; DFS HR = 4.7, P = 0.031) and LGG (OS HR = 1.8, P = 0.0024; DFS HR = 2, P = 1.60e-05) (Figure 2A and 2B), whereas it was associated with better prognosis in KIRC (OS HR = 0.63, P = 0.0035; DFS HR = 0.63, P = 0.012). In addition, high YTHDF2 expression was associated with poorer OS but not poorer DFS in LIHC (OS HR = 1.6, P = 0.0068; DFS HR = 1.3, P = 0.081) (Figure 2C and 2D) and SARC (OS HR = 2.1, P = 0.00044; DFS HR = 1.3, P = 0.16) (Figure 2E and 2F), whereas it was associated with superior OS but not superior DFS in UCEC (OS HR = 0.48, P = 0.045; DFS HR = 0.63, P = 1.6). In the TIMER database, higher YTHDF2 expression was associated with poor OS in KICH (HR = 24.208, 95% confidence interval [CI] = 2.122-276.177, P = 0.01), LGG (HR = 2.749, 95% CI = 1.697-4.453, P = 0), LIHC (HR = 2.194, 95% CI = 1.334-3.608, P = 0.002), and SARC (HR = 3.024, 95% CI = 1.725-5.302, P = 0). In the OncoLnc database, high YTHDF2 expression was

associated with poor prognosis in LGG (Cox coefficient = 0.329, P = 0.00038), LIHC (Cox coefficient = 0.316, P = 0.00088) and SARC (Cox coefficient = 0.428, P = 0.00012), whereas it was associated with superior prognosis in READ (Cox coefficient = -0.53, P = 0.022). In the Kaplan-Meier plotter database, high YTHDF2 expression was associated with poor OS in LIHC (HR = 2.71, 95% CI = 1.9-3.87, P = 1.00e-08) and SARC (HR = 2.71, 95% CI = 1.62-4.55, P = 8.20e-05), whereas it was associated with superior OS in BLCA (HR = 0.69, 95% CI = 0.51-0.92, P = 0.011), KIRC (HR = 0.58, 95% CI = 0.43-0.78, P = 0.00029), LUAD (HR = 0.67, 95% CI = 0.5-0.9, P = 0.0078), OV (HR = 0.73, 95% CI = 0.56-0.95, P = 0.021), READ (HR = 0.47, 95% CI = 0.22-1.01, P = 0.048), and THYM (HR = 0, 95% CI = 0-inf, P = 0.038). These results suggest that YTHDF2 is a potential prognostic biomarker of LGG, LIHC, and SARC, and indicate the prognostic value of YTHDF2 expression may depend on cancer type.

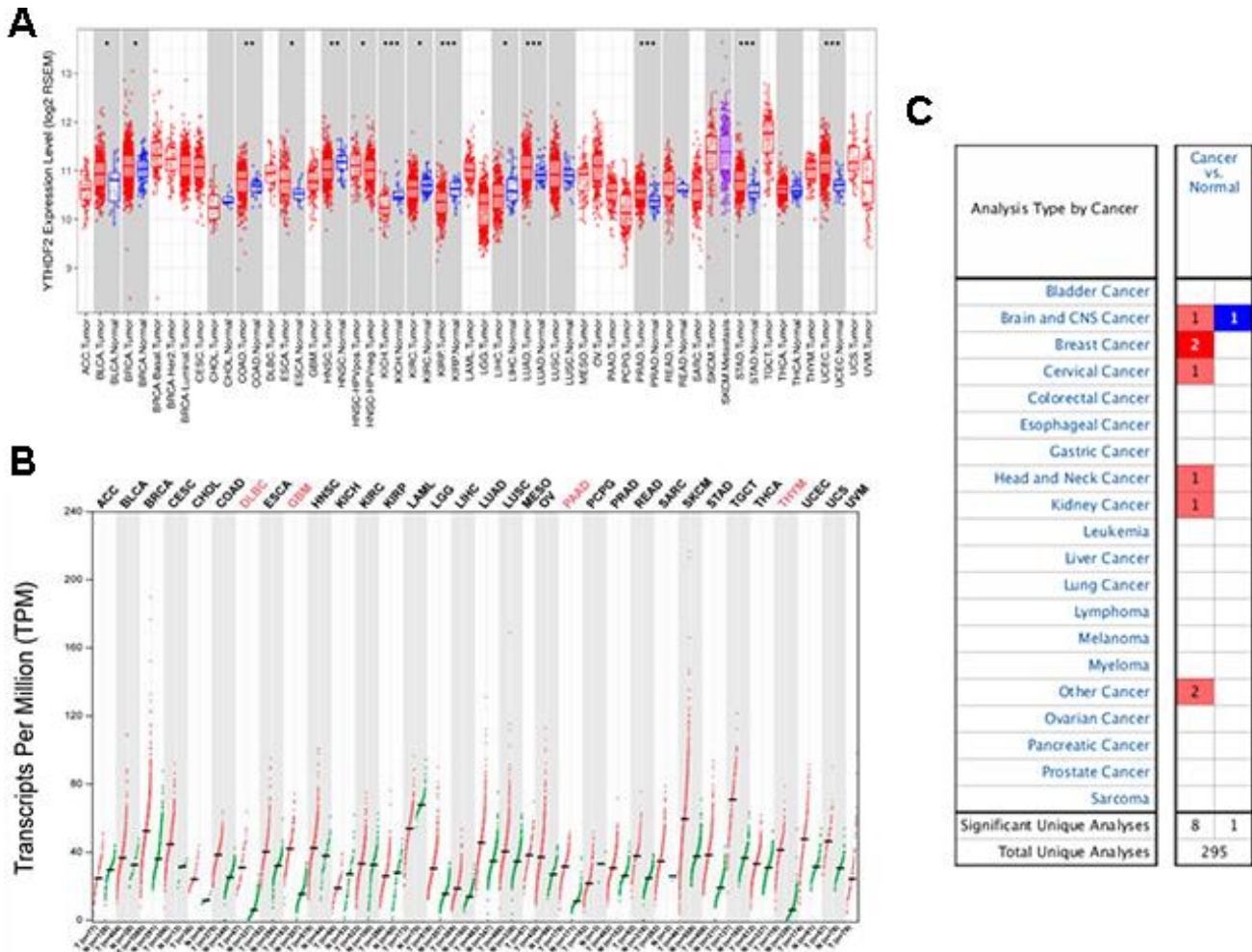


Figure 1. YTHDF2 expression in different types of human cancers were determined with (A) the TIMER, (B) GEPIA, and (C) ONCOMINE databases. ***P<0.001, **P<0.01, *P<0.05.

We then used the “survival” TIMER module to confirm the prognostic value of YTHDF2 expression in LGG, LIHC, and SARC (Table 1). We explored the clinical impact of YTHDF2 and corrected for potential confounding factors with a multivariable Cox proportional hazard model. In the univariate analysis, YTHDF2, patient age, and all TIICs (B cells, CD4+ T cells, CD8+ T cells, macrophages, neutrophils, and DCs) had a significant impact on OS in LGG.

YTHDF2, macrophages, and neutrophils had a significant impact on OS in LIHC, whereas YTHDF2, patient age, and CD4+ T cells had a significant impact on OS in SARC. In the multivariate analysis, we observed significant associations of YTHDF2, patient age, and macrophages with OS in LGG. However, only YTHDF2 was associated with OS in LIHC. In addition, associations between YTHDF2, patient age, CD4+ T cells, and OS were observed in SARC. By using the

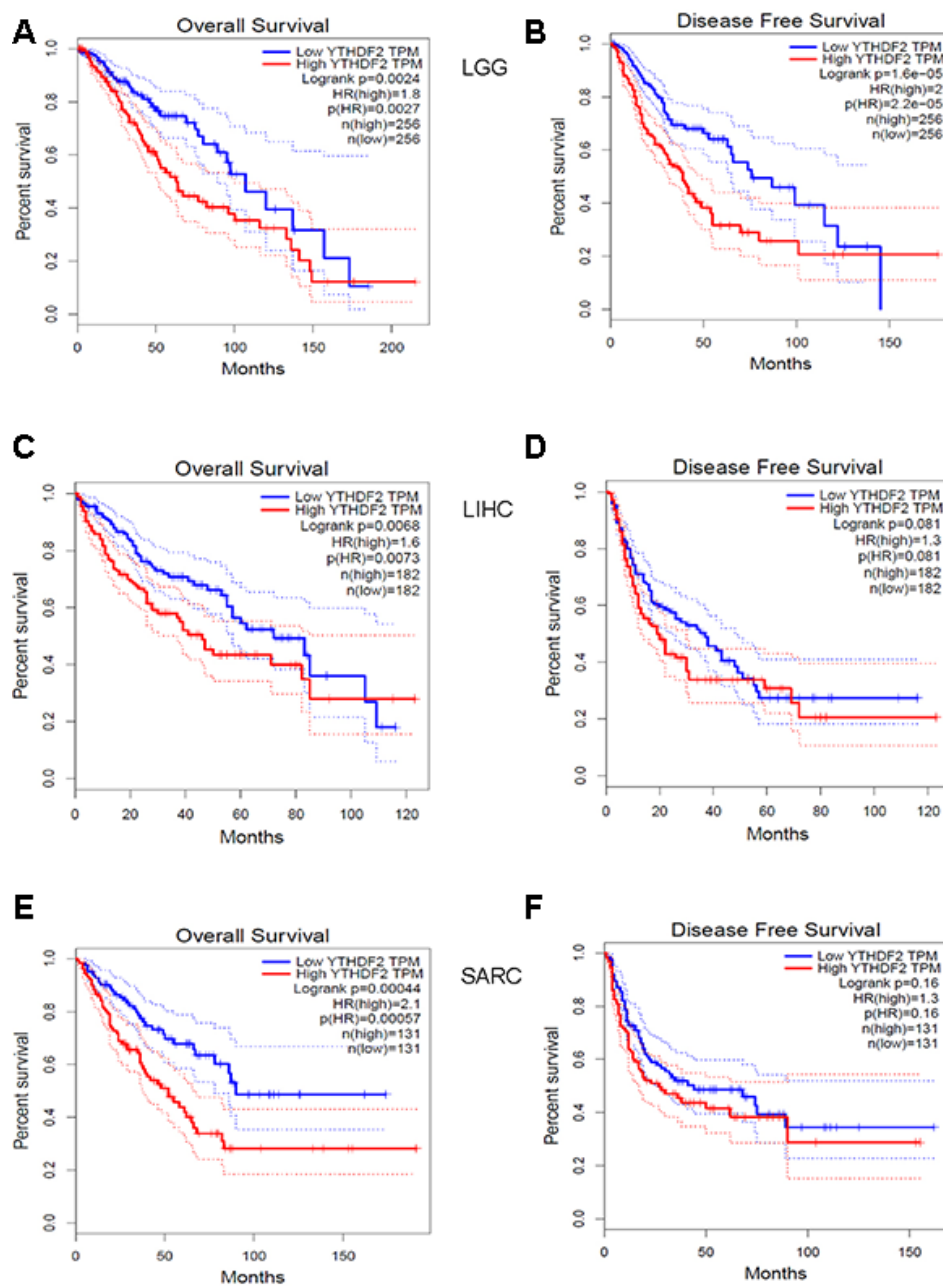


Figure 2. Kaplan-Meier survival curves comparing YTHDF2 high and low expression (A, B) in LGG, (C, D) LIHC, and (E, F) SARC in datasets from the GEPIA database. (A) OS and (B) DFS survival curves in LGG (n = 256). (C) OS and (D) DFS survival curves in LIHC (n = 182). (E) OS and (F) DFS survival curves in SARC (n = 131). DFS, disease-free survival; LGG, lower-grade glioma; LIHC, liver hepatocellular carcinoma; SARC, sarcoma; OS, overall survival.

Table 1. Univariate and multivariate analysis of association of YTHDF2 and prognostic factors with overall survival in LGG, LIHC and SARC.

Parameter	LGG				LIHC				SARC			
	Univariate analysis		Multivariate analysis		Univariate analysis		Multivariate analysis		Univariate analysis		Multivariate analysis	
	HR (95% CI)	P-value	HR (95% CI)	P-value	HR (95% CI)	P-value	HR (95% CI)	P-value	HR (95% CI)	P-value	HR (95% CI)	P-value
Age	1.058 (1.043-1.073)	***	1.057 (1.041-1.073)	***	1.01 (0.997-1.024)	0.139			1.019 (1.003-1.034)	*	1.019 (1.004-1.033)	*
gender (male)	1.092 (0.765-1.557)	0.629			0.816 (0.573-1.163)	0.26			0.87 (0.584 - 1.297)	0.494		
raceBlack	4939923 (0-Inf)	0.993			1.542 (0.656-3.622)	0.321			1.073 (0.130-8.821)	0.948		
raceWhite	3286235 (0-Inf)	0.993			1.300 (0.893-1.894)	0.172			0.788 (0.108-5.750)	0.814		
Tumor Purity	0.562 (0.25-1.261)	0.162			2.07 (0.901-4.759)	0.087			2.003 (0.723-5.551)	0.181		
B cell	830.428 (54.364-12685)	***	3.450 (0.011-1042.915)	0.671	0.864 (0.053-13.978)	0.918			0.224 (0.006-8.9)	0.426		
CD8+Tcell	19943.51 (1320.611-301181.6)	***	5.782 (0.005-6512.228)	0.625	0.515 (0.053-5.035)	0.569			0.677 (0.039-11.68)	0.788		
CD4+Tcell	47.835 (6.336-361.158)	***	0.062 (0.000-188.625)	0.497	11.602 (0.483-278.815)	0.131			0.016 (0.001-0.436)	*	0.016 (0.001-0.425)	*
Macrophage	296.664 (52.011-1692.124)	***	851.361 (15.430-46973.874)	**	22.634 (1.631-314.017)	*	23.940(0.535-1070.315)	0.101	0.41 (0.05-3.368)	0.407		
Neutrophil	881.918 (66.197-11749.39)	***	0.016 (0.000-49.469)	0.314	486.294 (2.269-104217.1)	*	0.299(0.000-2654.334)	0.795	0.003 (0-3.517)	0.107		
Dendritic	10.994 (4.24-28.506)	***	3.874 (0.095-157.366)	0.474	1.74 (0.54-5.612)	0.354			0.359 (0.088-1.475)	0.156		
YTHDF2	2.749 (1.697-4.453)	***	1.984 (1.104-3.565)	*	2.194 (1.334 -3.608)	**	2.094(1.270-3.454)	**	3.024 (1.725-5.302)	***	3.013 (1.720-5.277)	***

LGG, Brain Lower Grade Glioma; LIHC, Liver hepatocellular carcinoma; SARC, Sarcoma; YTHDF2, YTH N6-methyladenosine RNA binding protein 2; Cor, R value of Spearman's correlation; None, correlation without adjustment. Purity, correlation adjusted by purity. P-value Significant Codes: $0 \leq *** < 0.001 \leq ** < 0.01 \leq * < 0.05$.

UALCAN database, higher YTHDF2 expression was associated with poor OS in LGG, LIHC, and SARC. YTHDF2 expression also impacted the OS in LGG, LIHC, and SARC with different clinicopathological parameters, such as gender and tumor grade (Supplementary Figure 1 and Supplementary Table 4). Although YTHDF2 expression was not significantly higher in LGG compared with normal samples (Supplementary Figure 2A), we found that YTHDF2 expression was higher in astrocytoma than in oligo-astrocytoma and oligodendroglioma. YTHDF2 expression was higher in grade 3 LGG than in grade 2. In addition, higher YTHDF2 expression was associated with poor OS

in all LGG and LGG with astrocytoma, but not oligoastrocytoma and oligodendroglioma (Supplementary Figure 2 and Supplementary Table 4).

YTHDF2 expression is correlated with the immune infiltration level in LGG

As stated previously, some TIICs were independent predictors of survival in cancers (Table 1). Therefore, we investigated the correlation of YTHDF2 expression with immune infiltration levels in 32 cancer types from the TIMER database. The analysis showed that YTHDF2 expression was associated with tumor purity

in 14 cancer types and B cell infiltration levels in 10 cancer types. In addition, YTHDF2 expression was associated with CD8+ T cell levels in 12 cancer types, CD4+ T cell levels in 14 cancer types, macrophage levels in 14 cancer types, neutrophil levels in 12 cancer types, and DC levels in 12 cancer types (Supplementary Table 5).

YTHDF2 expression was positively correlated with the levels of infiltrating B cells ($r = 0.505$, $P = 2.45e-32$), CD8+ T cells ($r = 0.25$, $P = 3.02e-08$), CD4+ T cells ($r = 0.379$, $P = 1.09e-17$), macrophages ($r = 0.309$, $P = 6.79e-12$), neutrophils ($r = 0.468$, $P = 3.39e-27$), and DCs ($r = 0.489$, $P = 5.91e-30$) in LGG (Figure 3A). However, YTHDF2 expression was only associated with neutrophils in LIHC ($r = 0.159$, $P = 3.01e-03$) (Figure 3B), and YTHDF2 expression had no significant correlations with infiltrating immune cell levels in SARC (Figure 3C). These findings strongly indicate that YTHDF2 plays an important role in immune infiltration in LGG.

Correlation analysis between YTHDF2 expression and immune markers

To better understand the relationship between YTHDF2 and various infiltrating immune cells, we analyzed the correlations between YTHDF2 expression and the marker genes of different immune cells and functional T cells in LGG, LIHC, and SARC with the TIMER database. Table 2 shows YTHDF2 expression was associated with most marker genes of the various

immune and T cells in LGG. However, YTHDF2 expression was associated with only 14 markers in LIHC and 13 markers in SARC (Table 2).

Interestingly, YTHDF2 expression was associated with gene markers of B cells, monocytes, TAMs, M2 macrophages, DCs, and Th2 cells in LGG (Table 2). These findings indicate that YTHDF2 may play a specific role in the regulation of macrophage polarization in LGG. We further investigated the relationship between YTHDF2 and the related genes and markers of TAMs. This analysis showed that YTHDF2 expression was related to TAM-related genes and markers, such as CCL2, CSF1, CSF1R, EGF, STAT3, STAT6, IL-6, IL-10, TLR4, TGF β (TGFB1), LOX, PD-L1 (CD274), PD-L2 (PDCD1LG2), CD80, CD86, and MFGE8 (Table 3). Poor prognosis in LGG correlate with most TAM markers, including EGF, STAT3, STAT6, IL-6, IL-10, TGF β (TGFB1), LOX, PD-L1 (CD274), PD-L2 (PDCD1LG2), CD80, and CD86 (Supplementary Table 6). These results further reveal that YTHDF2 has a strong relationship with TAM infiltration. We also found a significant relationship between YTHDF2 and DC markers, such as HLA-DPB1, HLA-DQB1, HLA-DRA, HLA-DPA1, BDCA-1(CD1C), and CD11c (ITGAX). In addition, a significant correlation between YTHDF2 and TGF β (TGFB1) was observed in Treg cells, whereas TIM-3 (HAVCR2) correlate with T cell exhaustion (Table 2)., These results further suggest that YTHDF2 plays a role in immune escape in the LGG microenvironment.

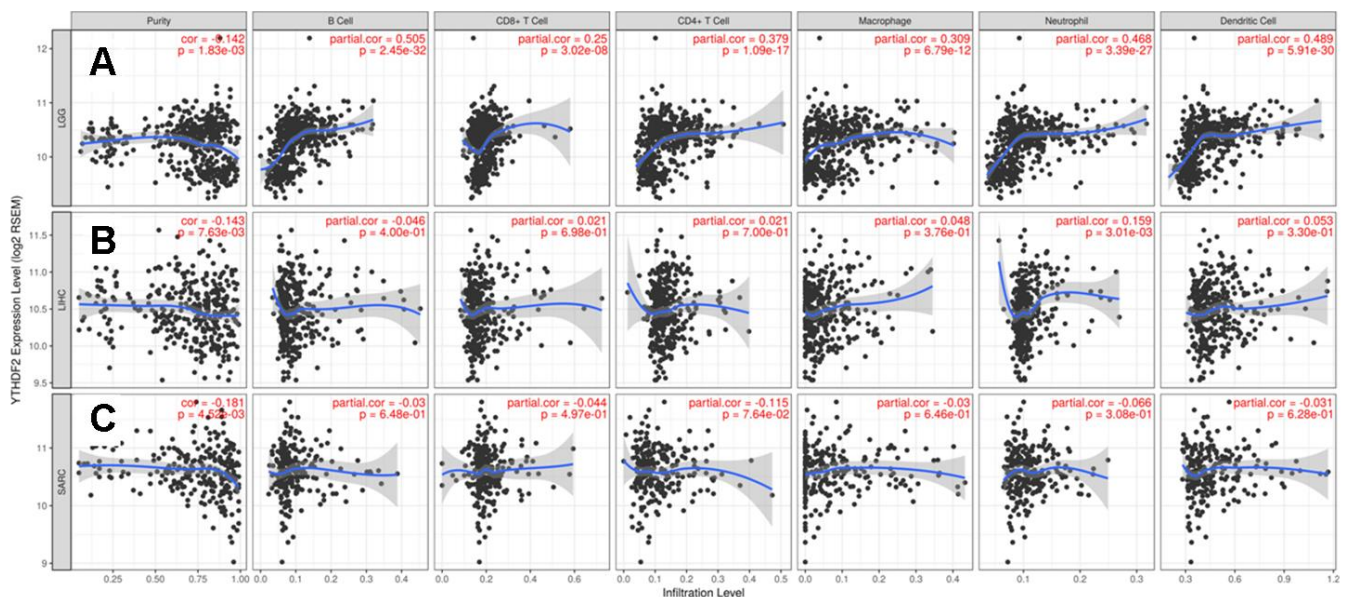


Figure 3. Correlation of YTHDF2 expression with immune infiltration level in (A) LGG, (B) LIHC, and (C) SARC. LGG, lower-grade glioma; LIHC, liver hepatocellular carcinoma; SARC, sarcoma.

Table 2. Correlation between YTHDF2 and relate genes and markers of immune cells in TIMER.

Description	Gene markers	LGG				LIHC				SARC			
		None		Purity		None		Purity		None		Purity	
		cor	p	cor	p	cor	p	cor	p	cor	p	cor	p
CD8+T cell	CD8A	0.090	*	0.083	0.069	0.042	0.042	0.023	0.669	0.007	0.914	-0.001	0.983
	CD8B	-0.077	0.081	-0.070	0.128	0.069	0.186	0.047	0.384	-0.030	0.625	-0.041	0.523
T cell(general)	CD3D	0.158	***	0.159	***	0.065	0.214	0.054	0.315	-0.033	0.594	-0.039	0.545
	CD3E	0.174	***	0.181	***	-0.018	0.732	-0.026	0.624	-0.081	0.191	-0.088	0.171
B cell	CD2	0.194	***	0.196	***	0.002	0.975	-0.012	0.829	-0.038	0.541	-0.045	0.478
	CD19	0.222	***	0.221	***	0.080	0.125	0.085	0.116	-0.045	0.472	-0.030	0.635
Monocyte	CD79A	0.273	***	0.304	***	-0.005	0.924	-0.016	0.773	0.016	0.802	0.031	0.632
	CD86	0.436	***	0.442	***	0.122	*	0.107	*	0.075	0.231	0.067	0.295
TAM	CSF1R	0.441	***	0.452	***	0.118	*	0.109	*	0.015	0.807	0.003	0.957
	CCL2	0.222	***	0.214	***	0.099	0.057	0.103	0.056	-0.065	0.297	-0.074	0.246
M1 Macrophage	CD68	0.344	***	0.344	***	0.093	0.073	0.089	0.100	0.115	0.065	0.113	0.078
	IL10	0.305	***	0.307	***	0.136	**	0.139	*	0.150	*	0.140	*
M2 Macrophage	INOS (NOS2)	-0.024	0.582	-0.014	0.758	-0.122	*	-0.113	*	0.043	0.488	0.044	0.491
	IRF5	0.357	***	0.364	***	-0.149	**	-0.155	**	-0.040	0.523	-0.028	0.667
Neutrophils	COX2 (PTGS2)	0.113	*	0.111	*	0.099	0.057	0.100	0.062	-0.026	0.677	-0.028	0.659
	CD163	0.221	***	0.210	***	0.110	*	0.104	0.054	0.084	0.178	0.073	0.254
Natural killer cell	VSIG4	0.426	***	0.420	***	0.145	**	0.139	*	0.091	0.145	0.078	0.222
	MS4A4A	0.296	***	0.302	***	0.121	*	0.112	*	0.053	0.396	0.036	0.576
Dendritic cell	CD66b (CEACAM8)	0.100	*	0.097	*	0.072	0.169	0.083	0.122	0.064	0.300	0.071	0.266
	CD11b (ITGAM)	0.435	***	0.441	***	0.133	*	0.138	*	0.015	0.810	0.004	0.950
Th1	CCR7	0.010	0.829	0.013	0.772	-0.010	0.855	-0.020	0.716	-0.170	**	-0.180	**
	KIR2DL1	0.003	0.946	0.000	0.996	0.088	0.092	0.092	0.088	-0.025	0.688	-0.038	0.549
Th2	KIR2DL3	0.085	0.055	0.086	0.059	0.078	0.132	0.082	0.130	-0.091	0.144	-0.106	0.097
	KIR2DL4	0.299	***	0.297	***	0.117	*	0.099	0.066	0.052	0.400	0.053	0.406
Tfh	KIR3DL1	-0.022	0.614	-0.029	0.520	0.067	0.195	0.059	0.273	-0.110	0.077	-0.134	*
	KIR3DL2	0.079	0.073	0.084	0.066	0.007	0.900	0.001	0.984	-0.037	0.555	-0.040	0.533
Treg	KIR3DL3	0.028	0.523	0.031	0.498	0.079	0.130	0.082	0.127	-0.074	0.235	-0.078	0.223
	KIR2DS4	0.038	0.386	0.045	0.323	0.065	0.209	0.076	0.156	-0.037	0.551	-0.036	0.578
Th17	HLA-DPB1	0.304	***	0.312	***	0.045	0.389	0.029	0.591	-0.050	0.423	-0.059	0.359
	HLA-DQB1	0.258	***	0.258	***	0.051	0.324	0.031	0.565	-0.017	0.787	-0.025	0.695
Treg	HLA-DRA	0.362	***	0.366	***	0.090	0.082	0.080	0.139	-0.012	0.846	-0.023	0.722
	HLA-DPA1	0.301	***	0.307	***	0.075	0.150	0.063	0.239	-0.063	0.309	-0.073	0.255
Treg	BDC4-1(CD1C)	0.135	**	0.139	**	-0.067	0.198	-0.065	0.226	-0.238	***	-0.257	***
	BDC4-4(NRP1)	0.014	0.755	-0.003	0.948	0.101	0.051	0.109	*	0.135	*	0.127	*
Treg	CD11c (ITGAX)	0.243	***	0.242	***	0.081	0.120	0.079	0.140	0.056	0.365	0.052	0.418
	T-bet (TBX21)	0.121	**	0.112	*	0.053	0.306	0.046	0.390	-0.073	0.238	-0.082	0.202
Treg	STAT4	-0.109	*	-0.103	*	-0.011	0.838	-0.022	0.679	0.005	0.941	-0.001	0.991
	STAT1	0.268	***	0.250	***	-0.010	0.841	-0.035	0.517	-0.148	*	-0.155	*
Treg	IFN-γ (IFNG)	0.112	*	0.130	**	0.097	0.061	0.086	0.112	0.026	0.681	0.025	0.693
	TNF-α (TNF)	0.166	***	0.175	***	0.116	*	0.120	*	0.054	0.385	0.031	0.628
Treg	GATA3	0.276	***	0.272	***	0.032	0.534	0.023	0.663	0.134	*	0.154	*
	STAT6	0.207	***	0.222	***	0.013	0.801	0.015	0.780	-0.350	***	-0.346	***
Treg	STAT5A	0.367	***	0.360	***	0.028	0.587	0.006	0.909	-0.183	**	-0.173	**
	IL13	0.047	0.283	0.045	0.322	0.027	0.607	0.032	0.548	0.039	0.533	0.064	0.321
Treg	BCL6	0.120	**	0.118	*	0.172	**	0.194	***	-0.164	**	-0.186	**
	IL21	0.100	*	0.089	0.053	0.063	0.223	0.057	0.289	-0.002	0.969	-0.009	0.885
Treg	STAT3	0.290	***	0.265	***	0.178	**	0.184	**	-0.248	***	-0.269	***
	IL17A	-0.030	0.497	-0.027	0.551	0.011	0.833	0.035	0.511	0.017	0.784	0.037	0.561
Treg	FOXP3	-0.322	***	-0.317	***	0.040	0.441	0.052	0.336	0.126	*	0.125	0.051
	TGFβ (TGFB1)	0.415	***	0.419	***	0.004	0.934	0.008	0.882	0.160	*	0.149	*
Treg	CCR8	0.028	0.531	0.020	0.662	0.070	0.181	0.075	0.166	0.064	0.305	0.050	0.436

T cell exhaustion	STAT5B	-0.021	0.640	-0.030	0.512	-0.205	***	-0.201	***	-0.459	***	-0.474	***
	PD-1 (PDCD1)	0.188	***	0.176	***	0.016	0.756	0.007	0.896	0.114	0.067	0.123	0.054
	CTLA4	0.167	***	0.175	***	0.048	0.355	0.031	0.562	0.010	0.878	0.012	0.849
	LAG3	0.187	***	0.189	***	0.032	0.536	0.009	0.861	0.103	0.097	0.113	0.078
	TIM-3 (HAVCR2)	0.458	***	0.457	***	0.162	**	0.153	**	0.106	0.090	0.100	0.118
	GZMB	0.034	0.442	0.036	0.430	0.039	0.451	0.025	0.637	0.123	*	0.119	0.063

LGG, Brain Lower Grade Glioma; LIHC, Liver hepatocellular carcinoma; SARC, Sarcoma; TAM, tumor-associated macrophage; Th, T helper cell; Tfh, Follicular helper T cell; Treg, regulatory T cell; Cor, R value of Spearman's correlation; None, correlation without adjustment. Purity, correlation adjusted by purity. P-value Significant Codes: 0 ≤ *** < 0.001 ≤ ** < 0.01 ≤ * < 0.05.

Table 3. Correlation analysis between YTHDF2 and relate genes and markers of TAMs in TIMER.

Description	Gene markers	LGG				LIHC				SARC			
		None		Purity		None		Purity		None		Purity	
		cor	p	cor	p	cor	p	cor	p	cor	p	cor	p
TAMs	CCL2	0.222	***	0.214	***	0.099	0.057	0.103	0.056	-0.065	0.297	-0.074	0.246
	CSF1	0.399	***	0.389	***	0.223	***	0.257	***	-0.010	0.874	-0.033	0.604
	CSF1R	0.441	***	0.452	***	0.118	*	0.109	*	0.015	0.807	0.003	0.957
	EGF	0.280	***	0.293	***	0.356	***	0.361	***	-0.185	**	-0.201	**
	STAT3	0.290	***	0.265	***	0.178	***	0.184	***	-0.248	***	-0.269	***
	STAT6	0.207	***	0.222	***	0.013	0.801	0.015	0.780	-0.350	***	-0.346	***
	IL6	0.318	***	0.303	***	0.028	0.593	0.037	0.490	0.056	0.369	0.038	0.554
	IL10	0.305	***	0.307	***	0.136	**	0.139	**	0.150	*	0.140	*
	TLR4	0.114	**	0.116	*	0.174	***	0.176	**	-0.092	0.138	-0.104	0.104
	TGFβ (TGFB1)	0.415	***	0.419	***	0.004	0.934	0.008	0.882	0.160	**	0.149	*
	LOX	0.478	***	0.466	***	0.090	0.083	0.111	*	0.191	**	0.187	**
	PD-L1(CD274)	0.198	***	0.189	***	0.192	***	0.195	***	-0.110	0.076	-0.123	0.054
	PD-L2(PDCD1LG2)	0.454	***	0.456	***	0.104	*	0.096	0.075	-0.014	0.823	-0.026	0.687
	CD80	0.300	***	0.277	***	0.153	**	0.154	**	0.121	0.052	0.117	0.069
	CD86	0.436	***	0.442	***	0.122	*	0.107	*	0.075	0.231	0.067	0.295
MFGE8	-0.366	***	-0.383	***	0.031	0.552	0.025	0.638	-0.433	***	-0.442	***	

LGG, Brain Lower Grade Glioma; LIHC, Liver hepatocellular carcinoma; SARC, Sarcoma; TAMs, tumor-associated macrophages; Cor, R value of Spearman's correlation; None, correlation without adjustment. Purity, correlation adjusted by purity. P-value Significant Codes: 0 ≤ *** < 0.001 ≤ ** < 0.01 ≤ * < 0.05.

YTHDF2 expression is correlated with IDH1 level in LGG

IDH1 mutations often occur in gliomas [47, 48] and AML [49, 50]. In addition, mutant IDH is highly associated with the regulation of the immune microenvironment in LGG [51]. Moreover, YTHDF2 is related to cancer stem cells (CSCs) in AML [52]. We attempted to find the relationship between YTHDF2 and IDH1 expression. We also analyzed the impact of the IDH1 mutation on immune infiltration levels in LGG. Interestingly, data from the GEPIA database showed that high IDH1 expression was associated with poor OS in LGG (HR = 1.7, P = 0.0061) (Figure 4A). LGG patients with IDH1 mutations had a superior OS according to the cBioPortal for Cancer Genomics

analysis (Figure 4B). Chinese Glioma Cooperative Group (CGGA) data also indicated that the IDH1 mutation led to a superior OS in glioma (Figure 4C). However, the IDH1 mutation had no impact on OS in AML (Figure 4D). In addition, YTHDF2 expression has a moderate positive relationship with IDH1 in LGG (Figure 4E) and a weak positive relationship with IDH1 in AML (Figure 4F). YTHDF2 expression was weakly related to TAM-related genes and markers in AML (Supplementary Table 7). More importantly, the levels of infiltration B cells, CD8+ T cells, macrophages, neutrophils, and DCs were higher in IDH1-wild-type LGG than IDH1-mutant LGG (Figure 4G). These results suggest that YTHDF2 may play an important role in immune infiltration in LGG, especially IDH1-wild-type LGG, but not in AML.

Enrichment analysis of YTHDF2 functional networks in LGG

We used the LinkedOmics database to analyze YTHDF2 mRNA sequencing data from 27 LGG patients. The volcano plot in Figure 5A shows that YTHDF2 was positively correlated with 241 genes (dark-red dots) but negatively correlated with 195 genes (dark-green dots) (FDR < 0.05). The 50 significant gene sets positively and negatively associated with YTHDF2 are shown in the heat map (Figure 5B and 5C). The LinkedOmics GESA tool was used to perform the Gene Ontology and pathway enrichment analyses (Supplementary Table 8 and Figure 5D–5G). Supplementary Table 8 shows that in general the

genes correlated with YTHDF2 were enriched in biological processes (double-strand break repair, DNA replication, cell cycle checkpoint, and mitotic cell cycle phase transition), cellular components (DNA packaging complex, protein-DNA complex, nuclear speck, replication fork, and chromosomal region), and molecular function (RNA polymerase II transcription factor binding, repressing transcription factor binding, NF-kappaB binding, nucleosome binding, and alcohol binding). Our results, demonstrating enrichment analyses for the KEGG, Panther, Reactome, and Wiki pathways, show the genes correlated with YTHDF2 were more enriched in cell cycle, TCA cycle, DNA replication, and the FAS signaling pathway.

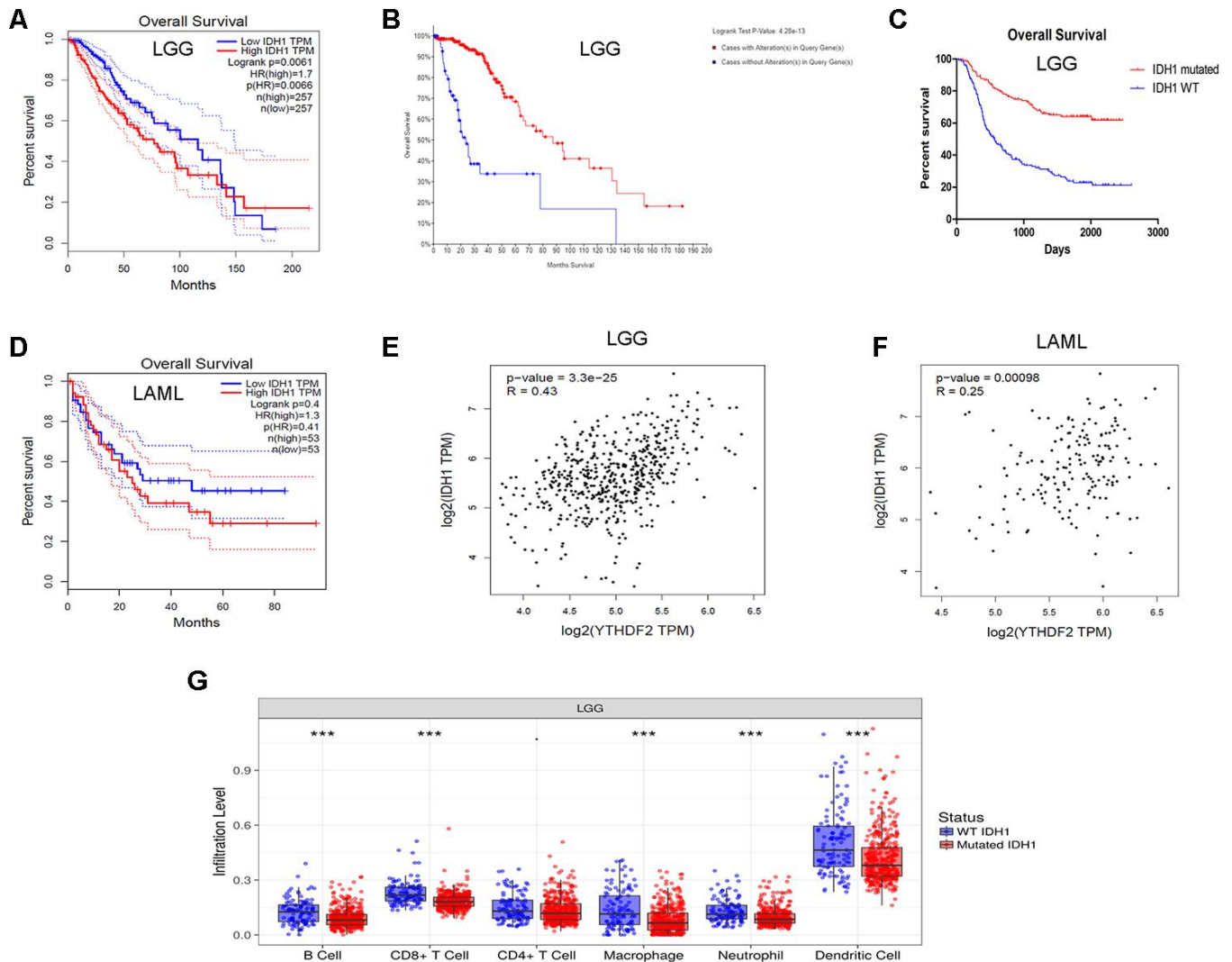


Figure 4. Correlation of YTHDF2 expression with IDH1 level in LGG. (A) High IDH1 expression was correlated with poor OS in the LGG GEPIA dataset. (B) LGG patients with IDH1 mutations had superior OS in the dataset from cBioPortal for Cancer Genomics. (C) IDH1 mutation led to a superior OS in gliomas. (D) IDH1 expression was not correlated with OS in the AML in GEPIA dataset. (E, F) YTHDF2 expression had a positive relationship with IDH1 in LGG and AML. (G) The immune infiltration levels were higher in IDH1-wild-type than in IDH1-mutant LGG. AML, acute myeloid leukemia; LGG, lower-grade glioma; OS, overall survival.

DISCUSSION

In the present study, we first performed a pan-cancer analysis to analyze YTHDF2 expression and prognostic value. Comprehensive analysis suggested that the differences in YTHDF2 expression and prognostic

values in different types of cancer may reflect underlying mechanisms associated with different biological characteristics. Importantly, multivariate analysis confirmed that high YTHDF2 expression was an independent prognostic factor in patients with LGG, LIHC, or SARC. We found that YTHDF2 expression

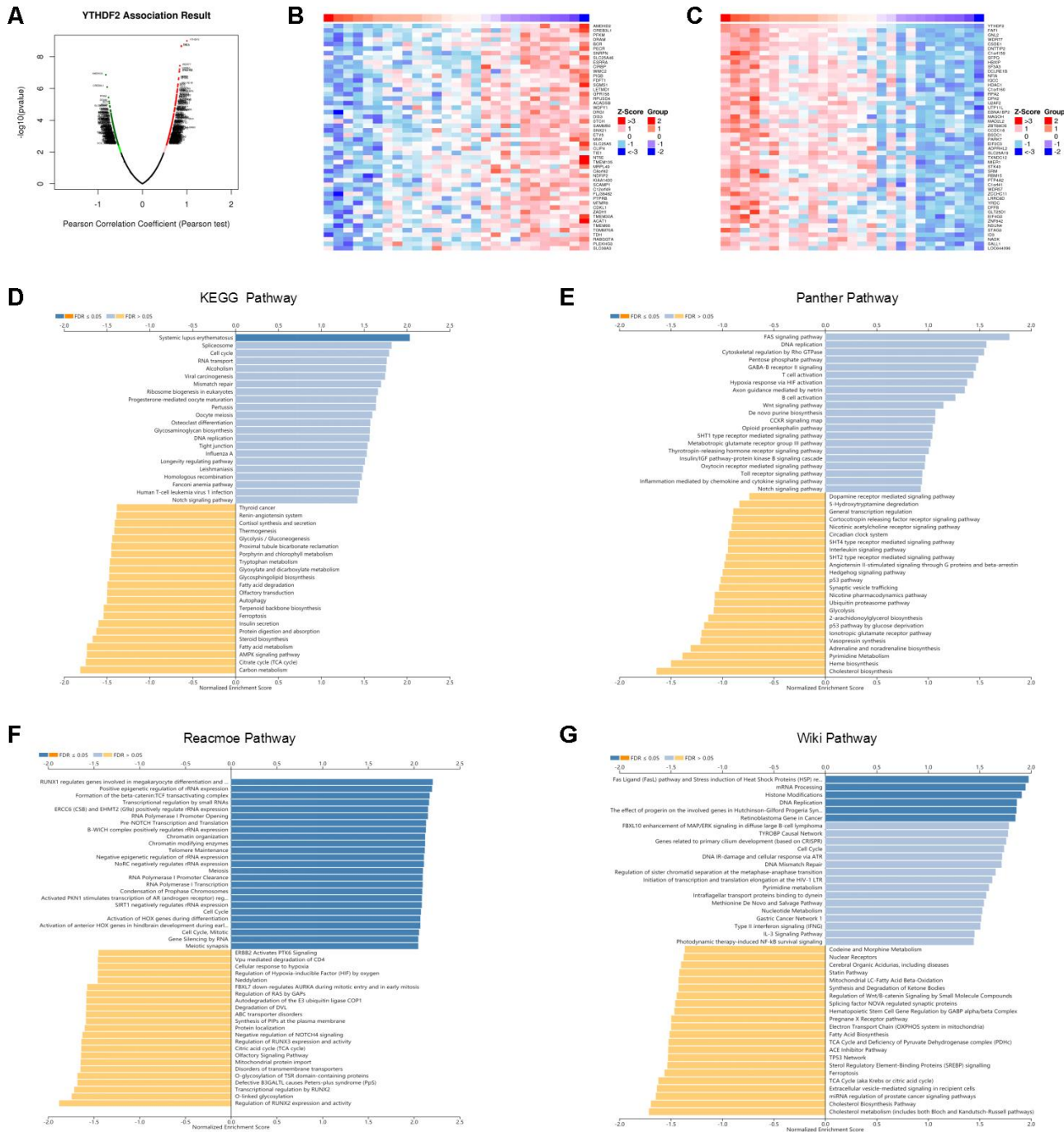


Figure 5. Enrichment analysis of YTHDF2 functional networks in LGG by LinkedOmics. (A) Volcano plot of genes differentially expressed in correlation with YTHDF2. **(B, C)** Heat maps of genes positively and negatively correlated with YTHDF2 (top 50). **(D)** KEGG pathway analysis of YTHDF2 by GSEA. **(E)** Panther pathway analysis of YTHDF2 by GSEA. **(F)** Reactome pathway analysis of YTHDF2 by GSEA. **(G)** Wiki pathway analysis of YTHDF2 by GSEA.

was higher in LGG compared with normal samples, although the difference was not significant. LGG are a diverse group of primary brain tumors, which mainly include astrocytoma, oligoastrocytoma, and oligodendroglioma. Previous studies have shown that astrocytic tumor type (vs. oligodendroglioma or oligodominant) was a poor prognostic indicator in patients with LGG [53–55]. We also found that YTHDF2 expression was higher in astrocytoma than in the other tumor types (oligoastrocytoma and oligodendroglioma). Moreover, high YTHDF2 expression was a prognostic factor in LGG with astrocytoma but not with oligoastrocytoma and oligodendroglioma. Similarly, the expression of YTHDF2 was higher in grade 3 LGG than in grade 2, and high YTHDF2 expression was a prognostic factor in LGG with different tumor grades. These results implied that YTHDF2 was a prognostic factor in LGG, especially with the more malignant subtype or higher tumor grade. However, more research is needed to verify the findings.

A second important finding from this study is that YTHDF2 expression positively correlated with the levels of infiltrating B cells, CD8+ T cells, CD4+ T cells, macrophages, neutrophils, and DCs in LGG. Notably, an association was found between YTHDF2 expression and TAM markers, such as CCL2, CSF1, CSF1R, EGF, STAT3, STAT6, IL-6, IL-10, TLR4, TGF β (TGFB1), LOX, PD-L1 (CD274), PD-L2 (PDCD1LG2), CD80, CD86, and MFGE8. TAMs play a special role in regulating different steps of tumor progression and metastasis [56]. In glioma, CSCs can induce M2 macrophages, which secrete many cytokines, including TGF- β 1 and IL-10, and facilitate immunosuppression [57]. Secretion of IL-10 and TGF- β was shown to facilitate an immunosuppressive microenvironment by inhibiting T cell proliferation in oral squamous cell carcinoma [58]. Interestingly, colony-stimulating factor-1 (CSF1) secreted from tumor cells was shown to induce macrophages to produce epidermal growth factor (EGF), which in turn promoted the migration of cancer cells [59]. In addition, inhibition of colony-stimulating factor-1 receptor (CSF1R) in TAMs suppressed the metastasis of pancreatic tumors [60]. The role of TAMs in immunosuppression has been widely studied. For instance, activation of the PD-1/PD-L1/PD-L2 and CTLA4/CD80/CD86 pathways leads to inhibition of TCR signal and T cell cytotoxic functions [61, 62]. Previously, it has been suggested that TAMs are attractive therapeutic targets, based on their important role in the tumor immunosuppressive microenvironment in cancer patients [56]. Another interesting finding is the association between YTHDF2 expression and DCs, Treg cells, and T cell exhaustion markers, such as HLA-DPB1, HLA-DQB1, HLA-DRA, HLA-DPA1, TGF β , and TIM-3. Notably, TIM-3 is a

crucial T cell exhaustion regulator [63]. DCs can promote tumor metastasis by increasing Treg cells and reducing CD8+T cell cytotoxicity [64]. In addition, some markers (tumor mutational burden [TMB], PD-1, and PD-L1) have been identified as the effectors of immunotherapy. TMB can be used as a biomarker to identify pediatric glioblastoma (GBM) patients who may benefit from immunotherapy [65]. However, another study found that high TMB is only found in 3.5% of GBM patients, and that IDH1-mutant gliomas are not enriched for high TMB [66]. PD-1 (PDCD1) promoter methylation is a prognostic factor in patients with LGG harboring IDH mutations [20]. A previous study found that PD-L2 expression upregulated in higher grade glioma and IDH-wild-type glioma. High PD-L2 expression was associated with poor survival in GBM [67]. Importantly, several immunotherapies have been evaluated in patients with glioma, including peptide vaccines, DC vaccines, oncolytic viruses, CAR-T cells, and checkpoint inhibitor therapy [68–70]. However, a previous study reported the response rates were low in refractory high-grade gliomas treated with PD-1 inhibitors [71]. TIGIT and PD-1 dual checkpoint blockade enhances antitumor immunity and survival in a murine GBM model [72]. Blocking PD-1/PD-L1 interactions together with MLN4924 therapy is a potential strategy for glioma treatment [73]. Gliomas treated with DC vaccination \pm murine anti-PD-1 monoclonal antibody blockade or a colony-stimulating factor 1 receptor inhibitor (PLX3397) had prolonged survival in vivo [74]. Previous studies indicate that combination therapy with immune checkpoint blockade is effective for the treatment of malignant tumors, including GBM [75, 76].

Our third important finding is that YTHDF2 expression correlated with IDH1 expression in LGG. The analysis showed that high IDH1 expression was associated with poor OS in LGG. IDH1 mutations were associated with a superior OS. This is consistent with previous studies showing that IDH1 mutation is an independent favorable prognostic marker in glioma [47, 48]. In addition, the immune infiltration levels were higher in IDH1-wild-type LGG than in IDH1-mutant LGG. We showed that significant infiltration of immune cells, such as B cells, CD8+ T cells, CD4+ T cells, macrophages, neutrophils, and DCs, was linked to poor prognosis in LGG. In a previous study, IDH-wild-type gliomas exhibit a more prominent tumor infiltrating lymphocytes than IDH-mutant cases [77]. IDH1 mutations in gliomas caused leukocyte chemotaxis downregulation, resulting in suppression of the tumor-associated immune system [78]. As previously noted, IDH-mutant gliomas can escape the immune surveillance of natural killer cells [79]. More importantly, YTHDF2 expression has a positive

relationship with IDH1 level. These results indicate that the role of YTHDF2 in immune infiltration in LGG may depend on IDH1 status. However, further investigations are needed to verify our findings.

Pathway enrichment analysis of YTHDF2 in LGG by GESA found that the genes correlated with YTHDF2 were more significantly enriched in cell cycle, TCA cycle, DNA replication, and the FAS signaling pathway. Interestingly, the most significant gene positively associated with YTHDF2, FAF1, can regulate antiviral immunity ([80, 81]). Moreover, notch family genes (the pathway found in the enrichment analysis) were prognostic biomarkers and correlated with immune infiltrates in gastric cancer ([82]). Because bioinformatics analysis was performed based on TCGA or GEO datasets, further biological experiments are needed to validate future results.

In summary, our data provide a comprehensive bioinformatics analysis of YTHDF2 expression and prognostic value in human cancers. High YTHDF2 expression correlates with poor prognosis and increased immune infiltration levels (including infiltration of B cells, CD8+ T cells, CD4+ T cells, macrophages, neutrophils and DCs) in LGG. YTHDF2 expression positively correlated with expression of several immune cell markers, including exhausted T cell markers, PD-1, TIM-3, and CTLA-4 in LGG. In addition, YTHDF2 expression positively correlated with TAM gene markers in LGG. Interestingly, YTHDF2 expression positively correlated with IDH1 expression in LGG. These findings suggest that YTHDF2 is a potential prognostic biomarker and correlates with tumor immune cells infiltration in LGG.

MATERIALS AND METHODS

GEPIA database analysis

GEPIA (<http://gepia.cancer-pku.cn/index.html>) [2] is an interactive web server for analyzing the RNA sequencing expression data of 9,736 tumors and 8,587 normal samples from the TCGA and the GTEx projects using a standard processing pipeline. GEPIA was used to analyze YTHDF2 expression and associated survival values (including OS and DFS) of YTHDF2 in 33 different cancer types. Using the Spearman method, correlation between YTHDF2 and IDH1 was determined. YTHDF2 values were represented on the x-axis, and IDH1 values were represented on the y-axis.

TIMER database analysis

The TIMER database (<https://cistrome.shinyapps.io/timer/>) [3], which includes 10,897 samples across 32 cancer types from TCGA, is a comprehensive resource for

estimating the abundance of six types of infiltrating immune cells, including B cells, CD4+ T cells, CD8+ T cells, neutrophils, macrophages, and DCs. We analyzed YTHDF2 expression in different cancer types via different expression modules and the correlation of YTHDF2 expression with the abundance of immune infiltrates via the gene module. Partial correlations between variables, when considering tumor purity, are shown on the left-most panel of the figure or table [83]. In addition, relationships between YTHDF2 expression and publicly available gene markers of TIICs were explored via correlation modules [84]. The Spearman method was used to determine the correlation coefficient.

ONCOMINE analysis

ONCOMINE (<http://www.oncomine.com>) [4], an online cancer microarray database, was applied to analyze YTHDF2 mRNA levels in different cancers. The search filters were set as the following: differential analysis (cancer vs normal), cancer type (breast cancer), sample type (clinical specimen), data type (mRNA), and gene (YTHDF2). Thresholds were set as gene rank, 10%; fold change, 2; and P-value, 0.05.

UALCAN database

UALCAN (<http://ualcan.path.uab.edu/index.html>) [5] is a portal for facilitating tumor subgroup gene expression and survival analyses. It was used to evaluate the mRNA levels and prognostic value of YTHDF2 in LGG patient and normal samples. A P value less than 0.05 was considered significant.

PrognoScan database analysis

The PrognoScan database (<http://www.abren.net/PrognoScan/>) [6] was used to analyze the relationships between YTHDF2 expression and patient prognosis, such as OS and DFS, across publicly available cancer microarray datasets.

Kaplan-Meier plotter database analysis

The Kaplan-Meier plotter (<http://kmplot.com/analysis/>) [7] is capable of assessing the effect of 54,675 genes on survival in 21 cancer types. The correlation between YTHDF2 expression and survival was analyzed by the pan-cancer module of the Kaplan-Meier plotter. The HR with 95% CI and the log-rank P-value were determined.

Oncolnc database analysis

Oncolnc (<http://www.oncolnc.org/>) [8] is an interactive tool for exploring survival correlations, and for downloading clinical data coupled to expression data

for mRNAs, miRNAs, and long noncoding RNAs. The correlation between YTHDF2 expression and survival was analyzed by OncoLnc. The Cox correlation coefficient and P-value were calculated.

CGGA database analysis

A total of 118 glioma samples (82 samples with IDH1 mutation and 37 with wild-type IDH1) from CGGA were analyzed to determine the association of IDH1 with survival [9]. GraphPad Prism software was used to generate a survival curve, and the log-rank test was used to assess the statistical significance.

cBioportal for Cancer Genomics database analysis

The cBioportal Cancer Genomics database (<https://www.cbioportal.org>) [10], which was originally developed at Memorial Sloan Kettering Cancer Center, enables users to visualize, analyze, and download large-scale cancer genomics datasets. The survival associated with IDH1 alterations in LGG was analyzed, and the log-rank test P-value was calculated. Determination of the correlation between YTHDF2 and IDH1 was performed using the Spearman and Pearson methods.

LinkedOmics dataset

LinkedOmics (<http://www.linkedomics.org/login.php>) [11] is a publicly available portal that includes multi-omics data from all 32 TCGA cancer types. It provides a unique platform for biologists and clinicians to access, analyze, and compare cancer multi-omics data within and across tumor types.

AUTHOR CONTRIBUTIONS

Xiangan Lin, Zhichao Wang, and Guangda Yang conceptualized the project. Xiangan Lin and Zhichao Wang helped to develop the methodology used in this manuscript. Xiangan Lin, Zhichao Wang, Guangda Yang, Guohua Wen, and Hailiang Zhang performed the investigations. Xiangan Lin, Guohua Wen, and Hailiang Zhang wrote the original draft of the manuscript. Zhichao Wang and Guangda Yang reviewed and edited the manuscript. Guohua Wen and Hailiang Zhang contributed to the manuscript preparation and creation. Guangda Yang and Guohua Wen supervised the project.

CONFLICTS OF INTEREST

The authors have no conflicts of interest to declare.

FUNDING

No funding was received for this project.

REFERENCES

1. Bray F, Ferlay J, Soerjomataram I, Siegel RL, Torre LA, Jemal A. Global cancer statistics 2018: GLOBOCAN estimates of incidence and mortality worldwide for 36 cancers in 185 countries. *CA Cancer J Clin.* 2018; 68:394–424. <https://doi.org/10.3322/caac.21492> PMID:30207593
2. Tang Z, Li C, Kang B, Gao G, Li C, Zhang Z. GEPIA: a web server for cancer and normal gene expression profiling and interactive analyses. *Nucleic Acids Res.* 2017; 45:W98–102. <https://doi.org/10.1093/nar/gkx247> PMID:28407145
3. Li T, Fan J, Wang B, Traugh N, Chen Q, Liu JS, Li B, Liu XS. TIMER: a web server for comprehensive analysis of tumor-infiltrating immune cells. *Cancer Res.* 2017; 77:e108–10. <https://doi.org/10.1158/0008-5472.CAN-17-0307> PMID:29092952
4. Rhodes DR, Yu J, Shanker K, Deshpande N, Varambally R, Ghosh D, Barrette T, Pandey A, Chinnaiyan AM. ONCOMINE: a cancer microarray database and integrated data-mining platform. *Neoplasia.* 2004; 6:1–6. [https://doi.org/10.1016/s1476-5586\(04\)80047-2](https://doi.org/10.1016/s1476-5586(04)80047-2) PMID:15068665
5. Chandrashekar DS, Bashel B, Balasubramanya SA, Creighton CJ, Ponce-Rodriguez I, Chakvarathi BV, Varambally S. UALCAN: a portal for facilitating tumor subgroup gene expression and survival analyses. *Neoplasia.* 2017; 19:649–58. <https://doi.org/10.1016/j.neo.2017.05.002> PMID:28732212
6. Mizuno H, Kitada K, Nakai K, Sarai A. PrognoScan: a new database for meta-analysis of the prognostic value of genes. *BMC Med Genomics.* 2009; 2:18. <https://doi.org/10.1186/1755-8794-2-18> PMID:19393097
7. Nagy Á, Lániczky A, Menyhárt O, Gyórfy B. Validation of miRNA prognostic power in hepatocellular carcinoma using expression data of independent datasets. *Sci Rep.* 2018; 8:9227. <https://doi.org/10.1038/s41598-018-27521-y> PMID:29907753
8. Anaya J. OncoLnc: linking TCGA survival data to mRNAs, miRNAs, and lncRNAs. *PeerJ Computer Science.* 2016. <https://doi.org/10.7717/peerj-cs.67>
9. Yan W, Zhang W, You G, Zhang J, Han L, Bao Z, Wang Y, Liu Y, Jiang C, Kang C, You Y, Jiang T. Molecular classification of gliomas based on whole genome gene expression: a systematic report of 225 samples from

- the Chinese glioma cooperative group. *Neuro Oncol.* 2012; 14:1432–40.
<https://doi.org/10.1093/neuonc/nos263>
PMID:[23090983](https://pubmed.ncbi.nlm.nih.gov/23090983/)
10. Gao J, Aksoy BA, Dogrusoz U, Dresdner G, Gross B, Sumer SO, Sun Y, Jacobsen A, Sinha R, Larsson E, Cerami E, Sander C, Schultz N. Integrative analysis of complex cancer genomics and clinical profiles using the cBioPortal. *Sci Signal.* 2013; 6:pl1.
<https://doi.org/10.1126/scisignal.2004088>
PMID:[23550210](https://pubmed.ncbi.nlm.nih.gov/23550210/)
 11. Vasaikar SV, Straub P, Wang J, Zhang B. LinkedOmics: analyzing multi-omics data within and across 32 cancer types. *Nucleic Acids Res.* 2018; 46:D956–63.
<https://doi.org/10.1093/nar/gkx1090> PMID:[29136207](https://pubmed.ncbi.nlm.nih.gov/29136207/)
 12. Werner JM, Schweinsberg V, Schroeter M, von Reutern B, Malter MP, Schlaak M, Fink GR, Mauch C, Galldiks N. Successful treatment of myasthenia gravis following PD-1/CTLA-4 combination checkpoint blockade in a patient with metastatic melanoma. *Front Oncol.* 2019; 9:84.
<https://doi.org/10.3389/fonc.2019.00084>
PMID:[30828569](https://pubmed.ncbi.nlm.nih.gov/30828569/)
 13. Brahmer JR, Govindan R, Anders RA, Antonia SJ, Sagorsky S, Davies MJ, Dubinett SM, Ferris A, Gandhi L, Garon EB, Hellmann MD, Hirsch FR, Malik S, et al. The society for immunotherapy of cancer consensus statement on immunotherapy for the treatment of non-small cell lung cancer (NSCLC). *J Immunother Cancer.* 2018; 6:75.
<https://doi.org/10.1186/s40425-018-0382-2>
PMID:[30012210](https://pubmed.ncbi.nlm.nih.gov/30012210/)
 14. Miksch RC, Schoenberg MB, Weniger M, Bösch F, Ormanns S, Mayer B, Werner J, Bazhin AV, D’Haese JG. Prognostic impact of tumor-infiltrating lymphocytes and neutrophils on survival of patients with upfront resection of pancreatic cancer. *Cancers (Basel).* 2019; 11:39.
<https://doi.org/10.3390/cancers11010039>
PMID:[30609853](https://pubmed.ncbi.nlm.nih.gov/30609853/)
 15. Zheng X, Song X, Shao Y, Xu B, Hu W, Zhou Q, Chen L, Zhang D, Wu C, Jiang J. Prognostic role of tumor-infiltrating lymphocytes in esophagus cancer: a meta-analysis. *Cell Physiol Biochem.* 2018; 45:720–32.
<https://doi.org/10.1159/000487164> PMID:[29414812](https://pubmed.ncbi.nlm.nih.gov/29414812/)
 16. Mielgo A, Schmid MC. Impact of tumour associated macrophages in pancreatic cancer. *BMB Rep.* 2013; 46:131–38.
<https://doi.org/10.5483/bmbrep.2013.46.3.036>
PMID:[23527856](https://pubmed.ncbi.nlm.nih.gov/23527856/)
 17. Bingle L, Brown NJ, Lewis CE. The role of tumour-associated macrophages in tumour progression: implications for new anticancer therapies. *J Pathol.* 2002; 196:254–65.
<https://doi.org/10.1002/path.1027> PMID:[11857487](https://pubmed.ncbi.nlm.nih.gov/11857487/)
 18. Goodman AM, Kato S, Bazhenova L, Patel SP, Frampton GM, Miller V, Stephens PJ, Daniels GA, Kurzrock R. Tumor mutational burden as an independent predictor of response to immunotherapy in diverse cancers. *Mol Cancer Ther.* 2017; 16:2598–608.
<https://doi.org/10.1158/1535-7163.MCT-17-0386>
PMID:[28835386](https://pubmed.ncbi.nlm.nih.gov/28835386/)
 19. Liu B, Arakawa Y, Yokogawa R, Tokunaga S, Terada Y, Murata D, Matsui Y, Fujimoto KI, Fukui N, Tanji M, Mineharu Y, Minamiguchi S, Miyamoto S. PD-1/PD-L1 expression in a series of intracranial germinoma and its association with Foxp3+ and CD8+ infiltrating lymphocytes. *PLoS One.* 2018; 13:e0194594.
<https://doi.org/10.1371/journal.pone.0194594>
PMID:[29617441](https://pubmed.ncbi.nlm.nih.gov/29617441/)
 20. Röver LK, Gevensleben H, Dietrich J, Bootz F, Landsberg J, Goltz D, Dietrich D. PD-1 (PDCD1) promoter methylation is a prognostic factor in patients with diffuse lower-grade gliomas harboring isocitrate dehydrogenase (IDH) mutations. *EBioMedicine.* 2018; 28:97–104.
<https://doi.org/10.1016/j.ebiom.2018.01.016>
PMID:[29396294](https://pubmed.ncbi.nlm.nih.gov/29396294/)
 21. Wang X, Guo G, Guan H, Yu Y, Lu J, Yu J. Challenges and potential of PD-1/PD-L1 checkpoint blockade immunotherapy for glioblastoma. *J Exp Clin Cancer Res.* 2019; 38:87.
<https://doi.org/10.1186/s13046-019-1085-3>
PMID:[30777100](https://pubmed.ncbi.nlm.nih.gov/30777100/)
 22. Wang D, Lin J, Yang X, Long J, Bai Y, Yang X, Mao Y, Sang X, Seery S, Zhao H. Combination regimens with PD-1/PD-L1 immune checkpoint inhibitors for gastrointestinal Malignancies. *J Hematol Oncol.* 2019; 12:42.
<https://doi.org/10.1186/s13045-019-0730-9>
PMID:[31014381](https://pubmed.ncbi.nlm.nih.gov/31014381/)
 23. Hsu MM, Balar AV. PD-1/PD-L1 combinations in advanced urothelial cancer: rationale and current clinical trials. *Clin Genitourin Cancer.* 2019; 17:e618–26.
<https://doi.org/10.1016/j.clgc.2019.03.009>
PMID:[31005473](https://pubmed.ncbi.nlm.nih.gov/31005473/)
 24. Zhao BS, Roundtree IA, He C. Post-transcriptional gene regulation by mRNA modifications. *Nat Rev Mol Cell Biol.* 2017; 18:31–42.
<https://doi.org/10.1038/nrm.2016.132>
PMID:[27808276](https://pubmed.ncbi.nlm.nih.gov/27808276/)
 25. Roundtree IA, Evans ME, Pan T, He C. Dynamic RNA modifications in gene expression regulation. *Cell.* 2017; 169:1187–200.

- <https://doi.org/10.1016/j.cell.2017.05.045>
PMID:[28622506](https://pubmed.ncbi.nlm.nih.gov/28622506/)
26. Deng X, Su R, Weng H, Huang H, Li Z, Chen J. RNA N⁶-methyladenosine modification in cancers: current status and perspectives. *Cell Res.* 2018; 28:507–17.
<https://doi.org/10.1038/s41422-018-0034-6>
PMID:[29686311](https://pubmed.ncbi.nlm.nih.gov/29686311/)
27. Zhang C, Fu J, Zhou Y. A review in research progress concerning m6A methylation and immunoregulation. *Front Immunol.* 2019; 10:922.
<https://doi.org/10.3389/fimmu.2019.00922>
PMID:[31080453](https://pubmed.ncbi.nlm.nih.gov/31080453/)
28. Lee M, Kim B, Kim VN. Emerging roles of RNA modification: m⁶A and u-tail. *Cell.* 2014; 158:980–87.
<https://doi.org/10.1016/j.cell.2014.08.005>
PMID:[25171402](https://pubmed.ncbi.nlm.nih.gov/25171402/)
29. Winkler R, Gillis E, Lasman L, Safra M, Geula S, Soyris C, Nachshon A, Tai-Schmiedel J, Friedman N, Le-Trilling VTK, Trilling M, Mandelboim M, Hanna JH, Schwartz S, Stern-Ginossar N. m6A modification controls the innate immune response to infection by targeting type I interferons. *Nat Immunol.* 2019; 20:173–182.
<https://doi.org/10.1038/s41590-018-0275-z>
PMID:[30559377](https://pubmed.ncbi.nlm.nih.gov/30559377/)
30. Yang S, Wei J, Cui YH, Park G, Shah P, Deng Y, Aplin AE, Lu Z, Hwang S, He C, He YY. m⁶A mRNA demethylase FTO regulates melanoma tumorigenicity and response to anti-PD-1 blockade. *Nat Commun.* 2019; 10:2782.
<https://doi.org/10.1038/s41467-019-10669-0>
PMID:[31239444](https://pubmed.ncbi.nlm.nih.gov/31239444/)
31. Wang H, Hu X, Huang M, Liu J, Gu Y, Ma L, Zhou Q, Cao X. Mettl3-mediated mRNA m⁶A methylation promotes dendritic cell activation. *Nat Commun.* 2019; 10:1898.
<https://doi.org/10.1038/s41467-019-09903-6>
PMID:[31015515](https://pubmed.ncbi.nlm.nih.gov/31015515/)
32. Han D, Liu J, Chen C, Dong L, Liu Y, Chang R, Huang X, Liu Y, Wang J, Dougherty U, Bissonnette MB, Shen B, Weichselbaum RR, et al. Anti-tumour immunity controlled through mRNA m⁶A methylation and YTHDF1 in dendritic cells. *Nature.* 2019; 566:270–74.
<https://doi.org/10.1038/s41586-019-0916-x>
PMID:[30728504](https://pubmed.ncbi.nlm.nih.gov/30728504/)
33. Chen YG, Chen R, Ahmad S, Verma R, Kasturi SP, Amaya L, Broughton JP, Kim J, Cadena C, Pulendran B, Hur S, Chang HY. N6-methyladenosine modification controls circular RNA immunity. *Mol Cell.* 2019; 76:96–109.e9.
<https://doi.org/10.1016/j.molcel.2019.07.016>
PMID:[31474572](https://pubmed.ncbi.nlm.nih.gov/31474572/)
34. Hesser CR, Karijovich J, Dominissini D, He C, Glaunsinger BA. N6-methyladenosine modification and the YTHDF2 reader protein play cell type specific roles in lytic viral gene expression during kaposi's sarcoma-associated herpesvirus infection. *PLoS Pathog.* 2018; 14:e1006995.
<https://doi.org/10.1371/journal.ppat.1006995>
PMID:[29659627](https://pubmed.ncbi.nlm.nih.gov/29659627/)
35. Liao S, Sun H, Xu C. YTH domain: a family of N⁶-methyladenosine (m⁶A) readers. *Genomics Proteomics Bioinformatics.* 2018; 16:99–107.
<https://doi.org/10.1016/j.gpb.2018.04.002>
PMID:[29715522](https://pubmed.ncbi.nlm.nih.gov/29715522/)
36. Yang Z, Li J, Feng G, Gao S, Wang Y, Zhang S, Liu Y, Ye L, Li Y, Zhang X. MicroRNA-145 modulates N⁶-methyladenosine levels by targeting the 3'-untranslated mRNA region of the N⁶-methyladenosine binding YTH domain family 2 protein. *J Biol Chem.* 2017; 292:3614–23.
<https://doi.org/10.1074/jbc.M116.749689>
PMID:[28104805](https://pubmed.ncbi.nlm.nih.gov/28104805/)
37. Zhong L, Liao D, Zhang M, Zeng C, Li X, Zhang R, Ma H, Kang T. YTHDF2 suppresses cell proliferation and growth via destabilizing the EGFR mRNA in hepatocellular carcinoma. *Cancer Lett.* 2019; 442:252–61.
<https://doi.org/10.1016/j.canlet.2018.11.006>
PMID:[30423408](https://pubmed.ncbi.nlm.nih.gov/30423408/)
38. Li J, Meng S, Xu M, Wang S, He L, Xu X, Wang X, Xie L. Downregulation of N⁶-methyladenosine binding YTHDF2 protein mediated by miR-493-3p suppresses prostate cancer by elevating N⁶-methyladenosine levels. *Oncotarget.* 2017; 9:3752–64.
<https://doi.org/10.18632/oncotarget.23365>
PMID:[29423080](https://pubmed.ncbi.nlm.nih.gov/29423080/)
39. Chen J, Sun Y, Xu X, Wang D, He J, Zhou H, Lu Y, Zeng J, Du F, Gong A, Xu M. YTH domain family 2 orchestrates epithelial-mesenchymal transition/proliferation dichotomy in pancreatic cancer cells. *Cell Cycle.* 2017; 16:2259–71.
<https://doi.org/10.1080/15384101.2017.1380125>
PMID:[29135329](https://pubmed.ncbi.nlm.nih.gov/29135329/)
40. French PJ, Swagemakers SM, Nagel JH, Kouwenhoven MC, Brouwer E, van der Spek P, Luiders TM, Kros JM, van den Bent MJ, Sillevis Smitt PA. Gene expression profiles associated with treatment response in oligodendrogliomas. *Cancer Res.* 2005; 65:11335–44.
<https://doi.org/10.1158/0008-5472.CAN-05-1886>
PMID:[16357140](https://pubmed.ncbi.nlm.nih.gov/16357140/)
41. Lee J, Kotliarova S, Kotliarov Y, Li A, Su Q, Donin NM, Pastorino S, Purow BW, Christopher N, Zhang W, Park JK, Fine HA. Tumor stem cells derived from glioblastomas cultured in bFGF and EGF more closely mirror the phenotype and genotype of primary tumors than do serum-cultured cell lines. *Cancer Cell.* 2006; 9:391–403.

<https://doi.org/10.1016/j.ccr.2006.03.030>

PMID:16697959

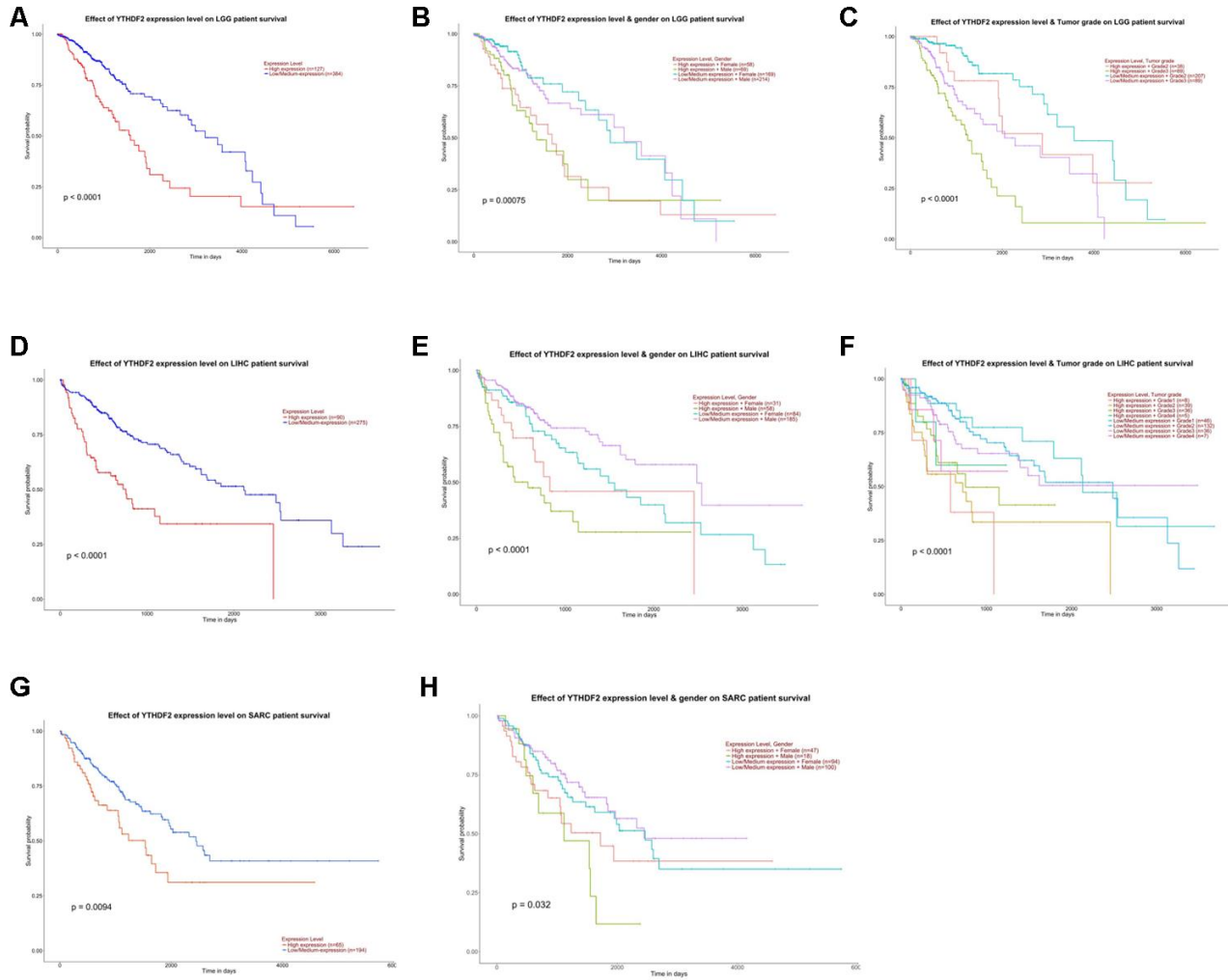
42. Sørli T, Perou CM, Tibshirani R, Aas T, Geisler S, Johnsen H, Hastie T, Eisen MB, van de Rijn M, Jeffrey SS, Thorsen T, Quist H, Matese JC, et al. Gene expression patterns of breast carcinomas distinguish tumor subclasses with clinical implications. *Proc Natl Acad Sci USA*. 2001; 98:10869–74.
<https://doi.org/10.1073/pnas.191367098>
PMID:11553815
43. Sorlie T, Tibshirani R, Parker J, Hastie T, Marron JS, Nobel A, Deng S, Johnsen H, Pesich R, Geisler S, Demeter J, Perou CM, Lønning PE, et al. Repeated observation of breast tumor subtypes in independent gene expression data sets. *Proc Natl Acad Sci USA*. 2003; 100:8418–23.
<https://doi.org/10.1073/pnas.0932692100>
PMID:12829800
44. Pyeon D, Newton MA, Lambert PF, den Boon JA, Sengupta S, Marsit CJ, Woodworth CD, Connor JP, Haugen TH, Smith EM, Kelsey KT, Turek LP, Ahlquist P. Fundamental differences in cell cycle deregulation in human papillomavirus-positive and human papillomavirus-negative head/neck and cervical cancers. *Cancer Res*. 2007; 67:4605–19.
<https://doi.org/10.1158/0008-5472.CAN-06-3619>
PMID:17510386
45. Yusenko MV, Kuiper RP, Boethe T, Ljungberg B, van Kessel AG, Kovacs G. High-resolution DNA copy number and gene expression analyses distinguish chromophobe renal cell carcinomas and renal oncocytomas. *BMC Cancer*. 2009; 9:152.
<https://doi.org/10.1186/1471-2407-9-152>
PMID:19445733
46. Morrison C, Farrar W, Kneile J, Williams N, Liu-Stratton Y, Bakaletz A, Aldred MA, Eng C. Molecular classification of parathyroid neoplasia by gene expression profiling. *Am J Pathol*. 2004; 165:565–76.
[https://doi.org/10.1016/S0002-9440\(10\)63321-4](https://doi.org/10.1016/S0002-9440(10)63321-4)
PMID:15277230
47. Sanson M, Marie Y, Paris S, Idbaih A, Laffaire J, Ducray F, El Hallani S, Boisselier B, Mokhtari K, Hoang-Xuan K, Delattre JY. Isocitrate dehydrogenase 1 codon 132 mutation is an important prognostic biomarker in gliomas. *J Clin Oncol*. 2009; 27:4150–54.
<https://doi.org/10.1200/JCO.2009.21.9832>
PMID:19636000
48. Juratli TA, Kirsch M, Geiger K, Klink B, Leinertz E, Pinzer T, Soucek S, Schrock E, Schackert G, Krex D. The prognostic value of IDH mutations and MGMT promoter status in secondary high-grade gliomas. *J Neurooncol*. 2012; 110:325–33.
<https://doi.org/10.1007/s11060-012-0977-2>
PMID:23015095
49. Schnittger S, Haferlach C, Ulke M, Alpermann T, Kern W, Haferlach T. IDH1 mutations are detected in 6.6% of 1414 AML patients and are associated with intermediate risk karyotype and unfavorable prognosis in adults younger than 60 years and unmutated NPM1 status. *Blood*. 2010; 116:5486–96.
<https://doi.org/10.1182/blood-2010-02-267955>
PMID:20805365
50. Paschka P, Schlenk RF, Gaidzik VI, Habdank M, Krönke J, Bullinger L, Späth D, Kayser S, Zucknick M, Götze K, Horst HA, Germing U, Döhner H, Döhner K. IDH1 and IDH2 mutations are frequent genetic alterations in acute myeloid leukemia and confer adverse prognosis in cytogenetically normal acute myeloid leukemia with NPM1 mutation without FLT3 internal tandem duplication. *J Clin Oncol*. 2010; 28:3636–43.
<https://doi.org/10.1200/JCO.2010.28.3762>
PMID:20567020
51. Qian Z, Li Y, Fan X, Zhang C, Wang Y, Jiang T, Liu X. Molecular and clinical characterization of IDH associated immune signature in lower-grade gliomas. *Oncoimmunology*. 2018; 7:e1434466.
<https://doi.org/10.1080/2162402X.2018.1434466>
PMID:29872572
52. Paris J, Morgan M, Campos J, Spencer GJ, Shmakova A, Ivanova I, Mapperley C, Lawson H, Wotherspoon DA, Sepulveda C, Vukovic M, Allen L, Sarapuu A, et al. Targeting the RNA m⁶A reader YTHDF2 selectively compromises cancer stem cells in acute myeloid leukemia. *Cell Stem Cell*. 2019; 25:137–48.e6.
<https://doi.org/10.1016/j.stem.2019.03.021>
PMID:31031138
53. Baumert BG, Stupp R, European Organization for Research and Treatment of Cancer (EORTC) Radiation Oncology Group, and European Organization for Research and Treatment of Cancer (EORTC) Brain Tumor Group. Low-grade glioma: a challenge in therapeutic options: the role of radiotherapy. *Ann Oncol*. 2008 (Suppl 7); 19:vii217–22.
<https://doi.org/10.1093/annonc/mdn434>
PMID:18790954
54. Pignatti F, van den Bent M, Curran D, Debruyne C, Sylvester R, Therasse P, Afra D, Cornu P, Bolla M, Vecht C, Karim AB, European Organization for Research and Treatment of Cancer Brain Tumor Cooperative Group, and European Organization for Research and Treatment of Cancer Radiotherapy Cooperative Group. Prognostic factors for survival in adult patients with cerebral low-grade glioma. *J Clin Oncol*. 2002; 20:2076–84.

- <https://doi.org/10.1200/JCO.2002.08.121>
PMID:11956268
55. Schiff D, Brown PD, Giannini C. Outcome in adult low-grade glioma: the impact of prognostic factors and treatment. *Neurology*. 2007; 69:1366–73.
<https://doi.org/10.1212/01.wnl.0000277271.47601.a1>
PMID:17893297
56. Aras S, Zaidi MR. TAMEless traitors: macrophages in cancer progression and metastasis. *Br J Cancer*. 2017; 117:1583–91.
<https://doi.org/10.1038/bjc.2017.356>
PMID:29065107
57. Wu A, Wei J, Kong LY, Wang Y, Priebe W, Qiao W, Sawaya R, Heimberger AB. Glioma cancer stem cells induce immunosuppressive macrophages/microglia. *Neuro Oncol*. 2010; 12:1113–25.
<https://doi.org/10.1093/neuonc/noq082>
PMID:20667896
58. Takahashi H, Sakakura K, Kudo T, Toyoda M, Kaira K, Oyama T, Chikamatsu K. Cancer-associated fibroblasts promote an immunosuppressive microenvironment through the induction and accumulation of protumoral macrophages. *Oncotarget*. 2017; 8:8633–47.
<https://doi.org/10.18632/oncotarget.14374>
PMID:28052009
59. Wyckoff J, Wang W, Lin EY, Wang Y, Pixley F, Stanley ER, Graf T, Pollard JW, Segall J, Condeelis J. A paracrine loop between tumor cells and macrophages is required for tumor cell migration in mammary tumors. *Cancer Res*. 2004; 64:7022–29.
<https://doi.org/10.1158/0008-5472.CAN-04-1449>
PMID:15466195
60. Mitchem JB, Brennan DJ, Knolhoff BL, Belt BA, Zhu Y, Sanford DE, Belaygorod L, Carpenter D, Collins L, Piwnica-Worms D, Hewitt S, Udupi GM, Gallagher WM, et al. Targeting tumor-infiltrating macrophages decreases tumor-initiating cells, relieves immunosuppression, and improves chemotherapeutic responses. *Cancer Res*. 2013; 73:1128–41.
<https://doi.org/10.1158/0008-5472.CAN-12-2731>
PMID:23221383
61. Kuang DM, Zhao Q, Peng C, Xu J, Zhang JP, Wu C, Zheng L. Activated monocytes in peritumoral stroma of hepatocellular carcinoma foster immune privilege and disease progression through PD-L1. *J Exp Med*. 2009; 206:1327–37.
<https://doi.org/10.1084/jem.20082173>
PMID:19451266
62. Ojalvo LS, King W, Cox D, Pollard JW. High-density gene expression analysis of tumor-associated macrophages from mouse mammary tumors. *Am J Pathol*. 2009; 174:1048–64.
<https://doi.org/10.2353/ajpath.2009.080676>
PMID:19218341
63. Mohammadizad H, Shahbazi M, Hasanjani Roushan MR, Soltanzadeh-Yamchi M, Mohammadnia-Afrouzi M. TIM-3 as a marker of exhaustion in CD8⁺ T cells of active chronic hepatitis B patients. *Microb Pathog*. 2019; 128:323–28.
<https://doi.org/10.1016/j.micpath.2019.01.026>
PMID:30660734
64. Sawant A, Hensel JA, Chanda D, Harris BA, Siegal GP, Maheshwari A, Ponnazhagan S. Depletion of plasmacytoid dendritic cells inhibits tumor growth and prevents bone metastasis of breast cancer cells. *J Immunol*. 2012; 189:4258–65.
<https://doi.org/10.4049/jimmunol.1101855>
PMID:23018462
65. Johnson A, Severson E, Gay L, Vergilio JA, Elvin J, Suh J, Daniel S, Covert M, Frampton GM, Hsu S, Lesser GJ, Stogner-Underwood K, Mott RT, et al. Comprehensive genomic profiling of 282 pediatric low- and high-grade gliomas reveals genomic drivers, tumor mutational burden, and hypermutation signatures. *Oncologist*. 2017; 22:1478–90.
<https://doi.org/10.1634/theoncologist.2017-0242>
PMID:28912153
66. Hodges TR, Ott M, Xiu J, Gatalica Z, Swensen J, Zhou S, Huse JT, de Groot J, Li S, Overwijk WW, Spetzler D, Heimberger AB. Mutational burden, immune checkpoint expression, and mismatch repair in glioma: implications for immune checkpoint immunotherapy. *Neuro Oncol*. 2017; 19:1047–57.
<https://doi.org/10.1093/neuonc/nox026>
PMID:28371827
67. Wang ZL, Li GZ, Wang QW, Bao ZS, Wang Z, Zhang CB, Jiang T. PD-L2 expression is correlated with the molecular and clinical features of glioma, and acts as an unfavorable prognostic factor. *Oncoimmunology*. 2018; 8:e1541535.
<https://doi.org/10.1080/2162402X.2018.1541535>
PMID:30713802
68. Dunn-Pirio AM, Vlahovic G. Immunotherapy approaches in the treatment of Malignant brain tumors. *Cancer*. 2017; 123:734–50.
<https://doi.org/10.1002/cncr.30371> PMID:27875627
69. Weant MP, Jesús CM, Yerram P. Immunotherapy in gliomas. *Semin Oncol Nurs*. 2018; 34:501–12.
<https://doi.org/10.1016/j.soncn.2018.10.011>
PMID:30396808
70. Desai R, Suryadevara CM, Batich KA, Farber SH, Sanchez-Perez L, Sampson JH. Emerging immunotherapies for glioblastoma. *Expert Opin Emerg Drugs*. 2016; 21:133–45.

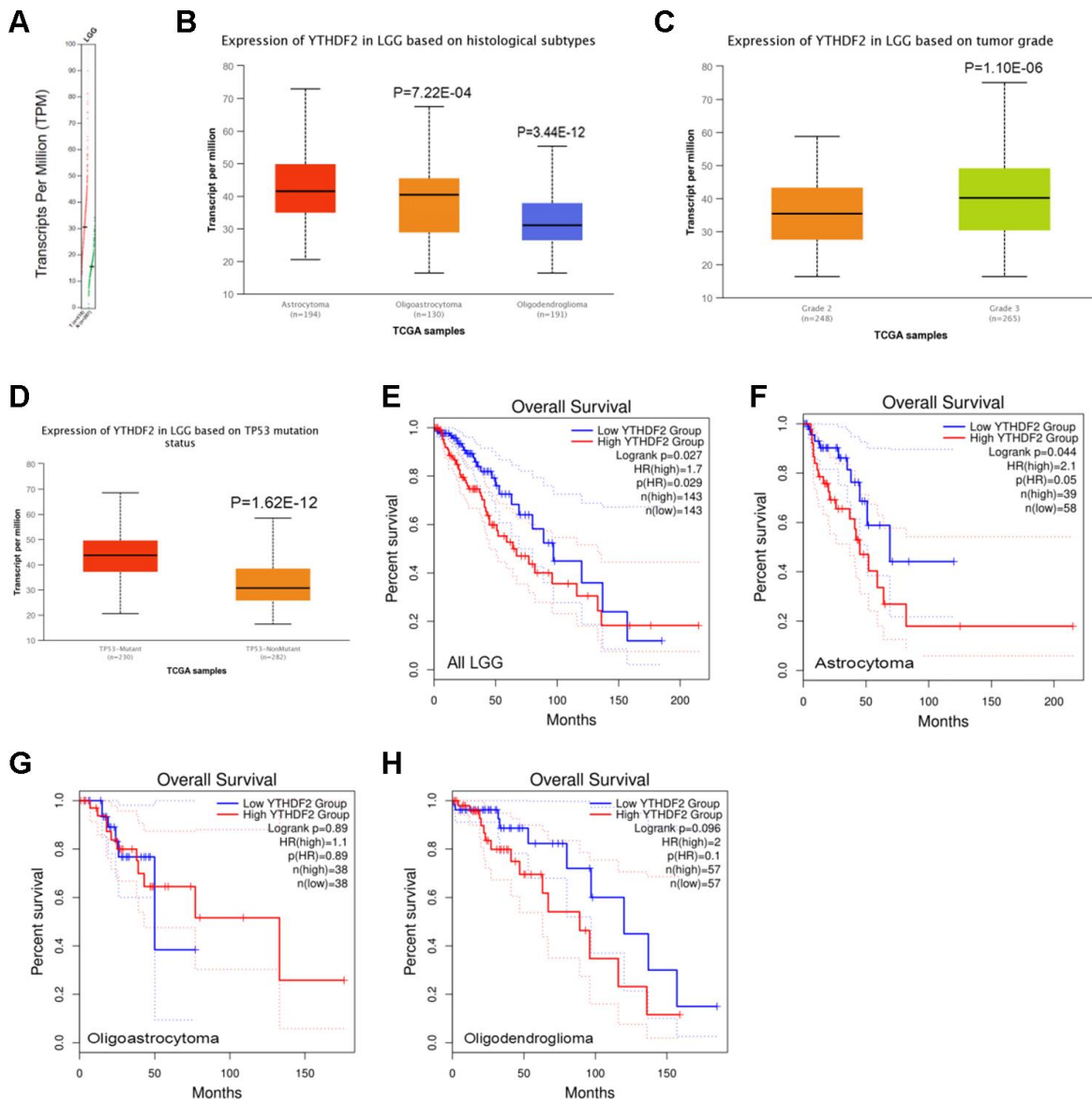
- <https://doi.org/10.1080/14728214.2016.1186643>
PMID:[27223671](https://pubmed.ncbi.nlm.nih.gov/27223671/)
71. Reiss SN, Yerram P, Modelevsky L, Grommes C. Retrospective review of safety and efficacy of programmed cell death-1 inhibitors in refractory high grade gliomas. *J Immunother Cancer*. 2017; 5:99.
<https://doi.org/10.1186/s40425-017-0302-x>
PMID:[29254497](https://pubmed.ncbi.nlm.nih.gov/29254497/)
72. Hung AL, Maxwell R, Theodros D, Belcaid Z, Mathios D, Luksik AS, Kim E, Wu A, Xia Y, Garzon-Muvdi T, Jackson C, Ye X, Tyler B, et al. TIGIT and PD-1 dual checkpoint blockade enhances antitumor immunity and survival in GBM. *Oncoimmunology*. 2018; 7:e1466769.
<https://doi.org/10.1080/2162402X.2018.1466769>
PMID:[30221069](https://pubmed.ncbi.nlm.nih.gov/30221069/)
73. Filippova N, Yang X, An Z, Nabors LB, Pereboeva L. Blocking PD1/PDL1 interactions together with MLN4924 therapy is a potential strategy for glioma treatment. *J Cancer Sci Ther*. 2018; 10:190–97.
<https://doi.org/10.4172/1948-5956.1000543>
PMID:[30393513](https://pubmed.ncbi.nlm.nih.gov/30393513/)
74. Antonios JP, Soto H, Everson RG, Moughon D, Orpilla JR, Shin NP, Sedighim S, Treger J, Odesa S, Tucker A, Yong WH, Li G, Cloughesy TF, et al. Immunosuppressive tumor-infiltrating myeloid cells mediate adaptive immune resistance via a PD-1/PD-L1 mechanism in glioblastoma. *Neuro Oncol*. 2017; 19:796–807.
<https://doi.org/10.1093/neuonc/now287>
PMID:[28115578](https://pubmed.ncbi.nlm.nih.gov/28115578/)
75. Wang JY, Bettgowda C. Genetics and immunotherapy: using the genetic landscape of gliomas to inform management strategies. *J Neurooncol*. 2015; 123:373–83.
<https://doi.org/10.1007/s11060-015-1730-4>
PMID:[25697584](https://pubmed.ncbi.nlm.nih.gov/25697584/)
76. Ishikawa E, Yamamoto T, Matsumura A. Prospect of immunotherapy for glioblastoma: tumor vaccine, immune checkpoint inhibitors and combination therapy. *Neurol Med Chir (Tokyo)*. 2017; 57:321–30.
<https://doi.org/10.2176/nmc.nmc.ra.2016-0334>
PMID:[28539528](https://pubmed.ncbi.nlm.nih.gov/28539528/)
77. Berghoff AS, Kiesel B, Widhalm G, Wilhelm D, Rajky O, Kurscheid S, Kresl P, Wöhrer A, Marosi C, Hegi ME, Preusser M. Correlation of immune phenotype with IDH mutation in diffuse glioma. *Neuro Oncol*. 2017; 19:1460–68.
<https://doi.org/10.1093/neuonc/now054>
PMID:[28531337](https://pubmed.ncbi.nlm.nih.gov/28531337/)
78. Amankulor NM, Kim Y, Arora S, Kargl J, Szulzewsky F, Hanke M, Margineantu DH, Rao A, Bolouri H, Delrow J, Hockenbery D, Houghton AM, Holland EC. Mutant IDH1 regulates the tumor-associated immune system in gliomas. *Genes Dev*. 2017; 31:774–86.
<https://doi.org/10.1101/gad.294991.116>
PMID:[28465358](https://pubmed.ncbi.nlm.nih.gov/28465358/)
79. Zhang X, Rao A, Sette P, Deibert C, Pomerantz A, Kim WJ, Kohanbash G, Chang Y, Park Y, Engh J, Choi J, Chan T, Okada H, et al. IDH mutant gliomas escape natural killer cell immune surveillance by downregulation of NKG2D ligand expression. *Neuro Oncol*. 2016; 18:1402–12.
<https://doi.org/10.1093/neuonc/now061>
PMID:[27116977](https://pubmed.ncbi.nlm.nih.gov/27116977/)
80. Dai T, Wu L, Wang S, Wang J, Xie F, Zhang Z, Fang X, Li J, Fang P, Li F, Jin K, Dai J, Yang B, et al. FAF1 regulates antiviral immunity by inhibiting MAVS but is antagonized by phosphorylation upon viral infection. *Cell Host Microbe*. 2018; 24:776–90.e5.
<https://doi.org/10.1016/j.chom.2018.10.006>
PMID:[30472208](https://pubmed.ncbi.nlm.nih.gov/30472208/)
81. Song S, Lee JJ, Kim HJ, Lee JY, Chang J, Lee KJ. Fas-associated factor 1 negatively regulates the antiviral immune response by inhibiting translocation of interferon regulatory factor 3 to the nucleus. *Mol Cell Biol*. 2016; 36:1136–51.
<https://doi.org/10.1128/MCB.00744-15>
PMID:[26811330](https://pubmed.ncbi.nlm.nih.gov/26811330/)
82. Hu J, Yu J, Gan J, Song N, Shi L, Liu J, Zhang Z, Du J. Notch1/2/3/4 are prognostic biomarker and correlated with immune infiltrates in gastric cancer. *Aging (Albany NY)*. 2020; 12:2595–609.
<https://doi.org/10.18632/aging.102764>
PMID:[32028262](https://pubmed.ncbi.nlm.nih.gov/32028262/)
83. Aran D, Sirota M, Butte AJ. Systematic pan-cancer analysis of tumour purity. *Nat Commun*. 2015; 6:8971.
<https://doi.org/10.1038/ncomms9971> PMID:[26634437](https://pubmed.ncbi.nlm.nih.gov/26634437/)
84. Pan JH, Zhou H, Cooper L, Huang JL, Zhu SB, Zhao XX, Ding H, Pan YL, Rong L. LAYN is a prognostic biomarker and correlated with immune infiltrates in gastric and colon cancers. *Front Immunol*. 2019; 10:6.
<https://doi.org/10.3389/fimmu.2019.00006>
PMID:[30761122](https://pubmed.ncbi.nlm.nih.gov/30761122/)

SUPPLEMENTARY MATERIALS

Supplementary Figures



Supplementary Figure 1. Prognostic YTHDF2 values in cancers analyzed by the UALCAN database. (A) LGG. **(B)** LGG with different gender. **(C)** LGG with different tumor grade. **(D)** LIHC. **(E)** LIHC with different gender. **(F)** LIHC with different tumor grade. **(G)** SARC. **(H)** SARC with different gender. LGG, lower-grade glioma; LIHC, liver hepatocellular carcinoma; SARC, sarcoma.



Supplementary Figure 2. Expression and overall survival of YTHDF2 in LGG analyzed by the UALCAN and GEPIA databases. (A) Expression level of YTHDF2 in LGG compared with normal sample. **(B)** Expression level of YTHDF2 in LGG based on histological subtypes. **(C)** Expression level of YTHDF2 in LGG based on tumor grade. **(D)** Expression level of YTHDF2 in LGG based on TP53 mutation status. **(E)** Overall survival of YTHDF2 in all LGG patients. **(F)** Overall survival of YTHDF2 in LGG patients with astrocytoma. **(G)** Overall survival of YTHDF2 in LGG patients with oligoastrocytoma. **(H)** Overall survival of YTHDF2 in LGG patients with oligodendroglioma. LGG, lower-grade glioma.

Supplementary Tables

Please browse Full Text version to see the data of Supplementary Tables 2, 3 and 5.

Supplementary Table 1. The significant Datasets of the YTHDF2 in Human Cancers (ONCOMINE database).

Cancer type	Sub cancer type	t-Test	Fold Change	P-value	Study
Brain and CNS Cancer	Anaplastic Oligoastrocytoma vs. Normal	5.874	2.433	1.90E-04	French Brain Statistics
	Glioblastoma vs. Normal	-16.491	-2.762	3.97E-13	Lee Brain Statistics
Breast cancer	Fibroadenoma vs. Normal	5.597	9.945	0.003	Sorlie Breast Statistics
	Fibroadenoma vs. Normal	6.235	11.69	0.002	Sorlie Breast 2 Statistics
Cervical Cancer	Cervical Cancer vs. Normal	6.66	2.061	3.58E-08	Pyeon Multi-cancer Statistics
Head and Neck cancer	Oral Cavity Carcinoma vs. Normal	5.523	2.838	1.78E-04	Pyeon Multi-cancer Statistics
Kidney cancer	Renal Wilms Tumor vs. Normal	4.817	2.3	0.002	Yusenko Renal Statistics
Other cancer	Parathyroid Hyperplasia vs. Normal	4.171	2.55	8.54E-04	Morrison Parathyroid Statistics
	Parathyroid Gland Adenoma vs. Normal	5.064	2.038	3.88E-04	Morrison Parathyroid Statistics

Supplementary Table 2. Prognostic values of YTHDF2 in cancers analyzed by the PrognosScan database.

Supplementary Table 3. Prognostic values of YTHDF2 in cancers analyzed by GEPIA, TIMER, OncoLnc, and Kaplan-Meier plotter.

Supplementary Table 4. The expression level and survival analysis of YTHDF2 with different clinicopathological characteristics in LGG, LIHC and SARC (UALCAN database).

Expression analysis	LGG		LIHC		SARC	
	P-value		P-value		P-value	
Sample Type						
Normal-vs-Primary tumor	NA		High	3.63E-12	Not sig	2.39E-01
Gender						
Normal-vs-Male	NA		high	8.52E-11	Not sig	3.05E-01
Normal-vs-Female	NA		high	4.73E-10	Not sig	1.90E-01
Male-vs-Female	Not sig	3.06E-01	Not sig	5.46E-01	high	4.22E-03
Tumor grade						
Normal-vs-Grade 1	NA		high	5.93E-05	NA	
Normal-vs-Grade 2	NA		high	4.07E-08	NA	
Normal-vs-Grade 3	NA		high	1.23E-11	NA	
Normal-vs-Grade 4	NA		high	1.89E-02	NA	
Grade 1-vs-Grade 2	NA		Not sig	8.68E-01	NA	
Grade 1-vs-Grade 3	NA		high	1.65E-02	NA	
Grade 1-vs-Grade 4	NA		Not sig	2.19E-01	NA	
Grade 2-vs-Grade 3	high	1.10E-06	high	7.18E-03	NA	
Grade 2-vs-Grade 4	NA		Not sig	8.90E-02	NA	
Grade 3-vs-Grade 4	NA			6.75E-01	NA	
TP53 mutation status						
Normal-vs-TP53-Mutant	NA		high	1.62E-12	Not sig	3.05E-01
Normal-vs-TP53-NonMutant	NA		high	1.63E-07	Not sig	2.09E-01
TP53-Mutant-vs-TP53-NonMutant	low	1.62E-12	low	1.06E-08	Not sig	8.60E-01
Histological subtypes						
Astrocytoma-vs-Oligoastrocytoma	low	7.22E-04	Normal-vs-N0	high	3.65E-12	NA
Astrocytoma-vs-Oligodendroglioma	low	3.44E-12	Normal-vs-N1	high	3.08E-03	NA
Oligoastrocytoma-vs-Oligodendroglioma	low	1.32E-03	N0-vs-N1	Not sig	8.31E-01	NA
Survival analysis						
Expression level	sig	P<0.0001	sig	P<0.0001	sig	P=0.0094
Tumor grade	sig	P<0.0001	sig	P<0.0001	NA	
Gender	sig	P=0.0075	sig	P<0.0001	sig	P=0.032

Note: LGG, Brain Lower Grade Glioma; LIHC, Liver hepatocellular carcinoma; SARC, Sarcoma; YTHDF2, YTH N6-methyladenosine RNA binding protein 2; high, means high expression; low, means low expression; sig, means significant; Not sig, means not significant; NA, means not available; Grade 1, Well differentiated (low grade); Grade 2, Moderately differentiated (intermediate grade); Grade 3, Poorly differentiated (high grade); Grade 4, Undifferentiated (high grade); N0, No regional lymph node metastasis; N1, Metastases in 1 to 3 axillary lymph nodes; N2, Metastases in 4 to 9 axillary lymph nodes; N3, Metastases in 10 or more axillary lymph nodes.

Supplementary Table 5. Correlation analysis between YTHDF2 and immune infiltration level in cancers by TIMER.

Supplementary Table 6. Prognostic values of relate genes and markers of TAMs in LGG analyzed by GEPIA.

Description	Gene markers	LGG			
		OS		DFS	
		HR	P-value	HR	P-value
TAM	CCL2	1.40	0.05100	1.00	0.96000
	CSF1	1.00	0.86000	1.20	0.32000
	CSF1R	1.20	0.37000	1.20	0.35000
	EGF	1.90	***	1.50	**
	STAT3	1.90	***	1.60	**
	STAT6	1.90	***	1.40	*
	IL6	1.90	***	1.40	*
	IL10	1.60	**	1.30	0.16000
	TLR4	1.00	0.94000	0.96	0.82000
	TGFβ (TGFB1)	1.70	**	1.50	**
	LOX	3.20	***	1.70	**
	PD-L1(CD274)	1.80	**	1.30	0.12000
	PD-L2(PDCD1LG2)	2.00	***	2.00	***
	CD80	2.50	***	1.60	**
	CD86	1.80	**	1.40	*
	MFGE8	1.10	0.68000	0.81	0.17000

LGG, Brain Lower Grade Glioma.P-value Significant Codes: 0 ≤ *** < 0.001 ≤ ** < 0.01 ≤ * < 0.05.

Supplementary Table 7. Correlation analysis between YTHDF2 and relate genes and markers of TAMs in LAML by GEPIA.

Description	Gene markers	LAML	
		Cor	p-value
TAMs	CCL2	-0.003	0.9700
	CSF1	0.240	**
	CSF1R	-0.018	0.8100
	EGF	0.210	**
	STAT3	0.430	***
	STAT6	0.230	**
	IL6	0.002	0.9800
	IL10	-0.079	0.3000
	TLR4	-0.028	0.7100
	TGFβ (TGFB1)	0.160	*
	LOX	0.270	***
	PD-L1(CD274)	0.200	**
	PD-L2(PDCD1LG2)	-0.035	0.6500
	CD80	0.280	***
	CD86	-0.240	**
	MFGE8	0.480	***

LAML, Acute Myeloid Leukemia; TAMs, tumor-associated macrophages; Cor, R value of Spearman's correlation; P-value Significant Codes: 0 ≤ *** < 0.001 ≤ ** < 0.01 ≤ * < 0.05.

Supplementary Table 8. The enrichment analysis of YTHDF2 in LGG by GSEA tool of LinkedOmics database.

Gene Set	Description	Size	P-Value	
BP	GO:0006302	double-strand break repair	56	0
	GO:0071166	ribonucleoprotein complex localization	41	0
	GO:0006260	DNA replication	90	0
	GO:0000075	cell cycle checkpoint	75	0
	GO:0044772	mitotic cell cycle phase transition	156	0
	GO:0006333	chromatin assembly or disassembly	55	0
	GO:0016458	gene silencing	55	0
	GO:0006338	chromatin remodeling	55	0

	GO:0040029	regulation of gene expression, epigenetic	75	0
	GO:0006403	RNA localization	75	0
CC	GO:0044815	DNA packaging complex	21	0
	GO:0032993	protein-DNA complex	58	0
	GO:0016607	nuclear speck	108	0
	GO:0005657	replication fork	25	0
	GO:0098687	chromosomal region	100	0
	GO:0035145	exon-exon junction complex	5	0.005
	GO:0017053	transcriptional repressor complex	25	0.012
	GO:0000793	condensed chromosome	61	0.008
	GO:0016605	PML body	32	0.011
	GO:0034399	nuclear periphery	51	0.004
MF	GO:0001085	RNA polymerase II transcription factor binding	51	0
	GO:0070491	repressing transcription factor binding	25	0
	GO:0051059	NF-kappaB binding	8	0
	GO:0031491	nucleosome binding	27	0
	GO:0043178	alcohol binding	24	0
	GO:0017056	structural constituent of nuclear pore	12	0.004
	GO:0035326	enhancer binding	43	0
	GO:0042826	histone deacetylase binding	35	0.007
	GO:0008327	methyl-CpG binding	9	0
	GO:0003714	transcription corepressor activity	74	0.004
KEGG Pathway	hsa04110	Cell cycle	46	0
	hsa03040	Spliceosome	40	0
	hsa03013	RNA transport	56	0
	hsa04152	AMPK signaling pathway	38	0
	hsa00020	Citrate cycle (TCA cycle)	9	0
	hsa05203	Viral carcinogenesis	63	0.004
	hsa03430	Mismatch repair	8	0.012
	hsa05166	Human T-cell leukemia virus 1 infection	81	0.025
	hsa03030	DNA replication	13	0.038
	Panther Pathway	P00020	FAS signaling pathway	17
P00014		Cholesterol biosynthesis	6	0.004
P00017		DNA replication	8	0.021
P02762		Pentose phosphate pathway	4	0.023
P02746		Heme biosynthesis	5	0.031
P00016		Cytoskeletal regulation by Rho GTPase	23	0.032
P00053		T cell activation	34	0.035
		RUNX1 regulates genes involved in megakaryocyte differentiation and platelet function	33	0
Reacmoe Pathway	R-HSA-8936459	Positive epigenetic regulation of rRNA expression	37	0
	R-HSA-5250913	RNA Polymerase I Promoter Opening	24	0
	R-HSA-73728	Formation of the beta-catenin:TCF transactivating complex	33	0
	R-HSA-201722	Chromatin modifying enzymes	74	0
	R-HSA-3247509	SIRT1 negatively regulates rRNA expression	26	0
	R-HSA-427359	Pre-NOTCH Transcription and Translation	34	0
	R-HSA-1912408	Cell Cycle	196	0
	R-HSA-1640170	Citric acid cycle (TCA cycle)	4	0.004
	R-HSA-71403	Negative regulation of NOTCH4 signaling	15	0.016
		Fas Ligand (FasL) pathway and Stress induction of Heat Shock	25	0
Wiki Pathway	WP314	Proteins (HSP) regulation	35	0
	WP411	mRNA Processing	32	0
	WP2446	Retinoblastoma Gene in Cancer	13	0
	WP466	DNA Replication	44	0
	WP179	Cell Cycle	4	0
	WP78	TCA Cycle (aka Krebs or citric acid cycle)	4	0

WP531	DNA Mismatch Repair	8	0.008
WP2453	TCA Cycle and Deficiency of Pyruvate Dehydrogenase complex (PDHc)	6	0.036
WP1742	TP53 Network	12	0.038
WP3664	Regulation of Wnt/B-catenin Signaling by Small Molecule Compounds	4	0.048

Note: LGG, Brain Lower Grade Glioma; YTHDF2, YTH N6-methyladenosine RNA binding protein 2; GSEA, Gene Set Enrichment Analysis; BP, biological process; CC, cellular component; MF, molecular function; GO, Gene Ontology; KEGG, Kyoto Encyclopedia of Genes and Genomes.